Space Sci Rev (2007) 129: 359–390
DOI 10.1007/s11214-007-9143-0

Solar Sources of Heliospheric Energetic Electron Events—Shocks or Flares?

S.W. Kahler

Received: 26 December 2006 / Accepted: 29 December 2006 /
Published online: 13 March 2007

Abstract Electrons with near-relativistic ($E \gtrsim 30$ keV, NrR) and relativistic ($E \gtrsim 0.3$ MeV) energies are often observed as discrete events in the inner heliosphere following solar transient activity. Several acceleration mechanisms have been proposed for the production of those electrons. One candidate is acceleration at MHD shocks driven by coronal mass ejections (CMEs) with speeds $\gtrsim$1000 km s^{-1}. Many NrR electron events are temporally associated only with flares while others are associated with flares as well as with CMEs or with radio type II shock waves. Since CME onsets and associated flares are roughly simultaneous, distinguishing the sources of electron events is a serious challenge. On a phenomenological basis two classes of solar electron events were known several decades ago, but recent observations have presented a more complex picture. We review early and recent observational results to deduce different electron event classes and their viable acceleration mechanisms, defined broadly as shocks versus flares. The NrR and relativistic electrons are treated separately. Topics covered are: solar electron injection delays from flare impulsive phases; comparisons of electron intensities and spectra with flares, CMEs and accompanying solar energetic proton (SEP) events; multiple spacecraft observations; two-phase electron events; coronal flares; shock-associated (SA) events; electron spectral invariance; and solar electron intensity size distributions. This evidence suggests that CME-driven shocks are statistically the dominant acceleration mechanism of relativistic events, but most NrR electron events result from flares. Determining the solar origin of a given NrR or relativistic electron event remains a difficult proposition, and suggestions for future work are given.

Keywords Acceleration of particles · Interplanetary medium · Sun: particle emission · Sun: radio radiation · Sun: coronal mass ejections

1 Introduction

The first comprehensive picture of energetic electron production at the Sun was synthesized by Wild et al. (1963), who combined their solar flare radio burst types I through V with X-

S.W. Kahler (✉)
Air Force Research Laboratory, VSBXS, 29 Randolph Rd., Hanscom AFB, MA 01731-3010, USA
e-mail: stephen.kahler@hanscom.af.mil

ray and Hα flare observations to deduce two separate phases of electron acceleration. The first phase was a succession of bursts, each lasting $\sim$1 second, of $\sim$100 keV electrons that traveled upward through the corona to produce the type III radio bursts, characterized by fast drifts to lower frequencies. In large flares energetic electrons from the first phase were Fermi accelerated to higher ($\lesssim$1 GeV) energies in a second phase, which was due to traveling MHD shocks set up by the energy release of the first phase. As the shocks propagated away from the Sun, they were observed as slow frequency-drift type II radio bursts.

In situ observations of NrR and relativistic electron events at 1 AU supported and refined this two-phase picture of solar electron production. Two classes of $E > 40$ keV electron events were clear (Lin 1970): 1) simple NrR electron events with cutoff energies $\lesssim$300 keV, produced in small flares accompanied by type III, microwave, and hard ($E > 20$ keV) X-ray bursts, and 2) proton–electron or "complex" events with relativistic electrons and energetic ($E > 10$ MeV) protons (SEPs), produced in large eruptive flares accompanied by type II and IV and intense microwave and hard X-ray bursts. Simple NrR electron events were associated with optical flares in the well connected W30° to W90° longitude range, and complex events with flares located from E30° to W90°. Thus, the two classes of energetic electron events at 1 AU were directly linked to the two phases of solar electron acceleration. Although it was later recognized that ions could also be accelerated along with electrons in impulsive phases (Forrest and Chupp 1983), this two-class picture for solar electron acceleration has endured for several decades. Today we have far more extensive electron and other space observations to test and explore this relatively simple paradigm. In the following we review the changes or modifications to the paradigm compelled by the more recent observations. In particular, we ask whether we still find only two phases of solar electron acceleration, and if so, whether the first phase is limited only to NrR electrons and the second phase only to relativistic electrons.

With advances in the capabilities of charged-particle detectors, heliospheric electron events are now observed from the thermal solar-wind (Gosling et al. 2003) to the relativistic (Sierks et al. 1997; Klassen et al. 2005) energy regimes (Fig. 1). The observed antisunward flows and velocity dispersions establish that these electrons are accelerated in or near the solar corona. Electrons and ions have long been known to be accelerated in solar flares (Hudson and Ryan 1995). The good correlation found between 4–8 MeV γ-ray line and $E > 50$ keV X-ray fluences in solar flares suggests that the $\sim$10 MeV ions and the $\sim$100 keV electrons producing those emissions in the solar atmosphere are accelerated in a common process (Cliver et al. 1994). A similar correlation between the 2.22 MeV neutron-capture line and $E > 300$ keV X-ray flare fluences in observations with the Ramaty High-Energy Solar Spectroscopic Imager (RHESSI) (Shih et al. 2006) also indicates a common acceleration mechanism for $E > 30$ MeV protons and $E > 300$ keV electrons in flares. Solar flares are therefore obvious candidates for sources of the energetic heliospheric electron events.

The energy for electron acceleration in flares is presumed to arise in coronal flare magnetic reconnection (Fig. 2; Hamilton et al. 2005), which gives rise to three general candidate acceleration mechanisms: direct electric fields, shocks, and turbulence (Bastian et al. 1998). Problems with both shock formation and electron acceleration at shocks in coronal flares (Miller et al. 1997) make shocks an unlikely choice for electron acceleration in the flare reconnection region. Stochastic acceleration of electrons by cascading MHD waves is considered to be a strong possibility (Miller et al. 1996, 1997; Miller 2000; Petrosian and Liu 2004). Electric field acceleration at magnetic reconnection sites in flares is a viable mechanism for both ions and electrons and is the subject of considerable 2-D (Litvinenko 2003) and 3-D (Dalla and Browning 2005, 2006; Litvinenko 2006) analyses. Power-law electron distributions extending to relativistic energies were found in recent simulations

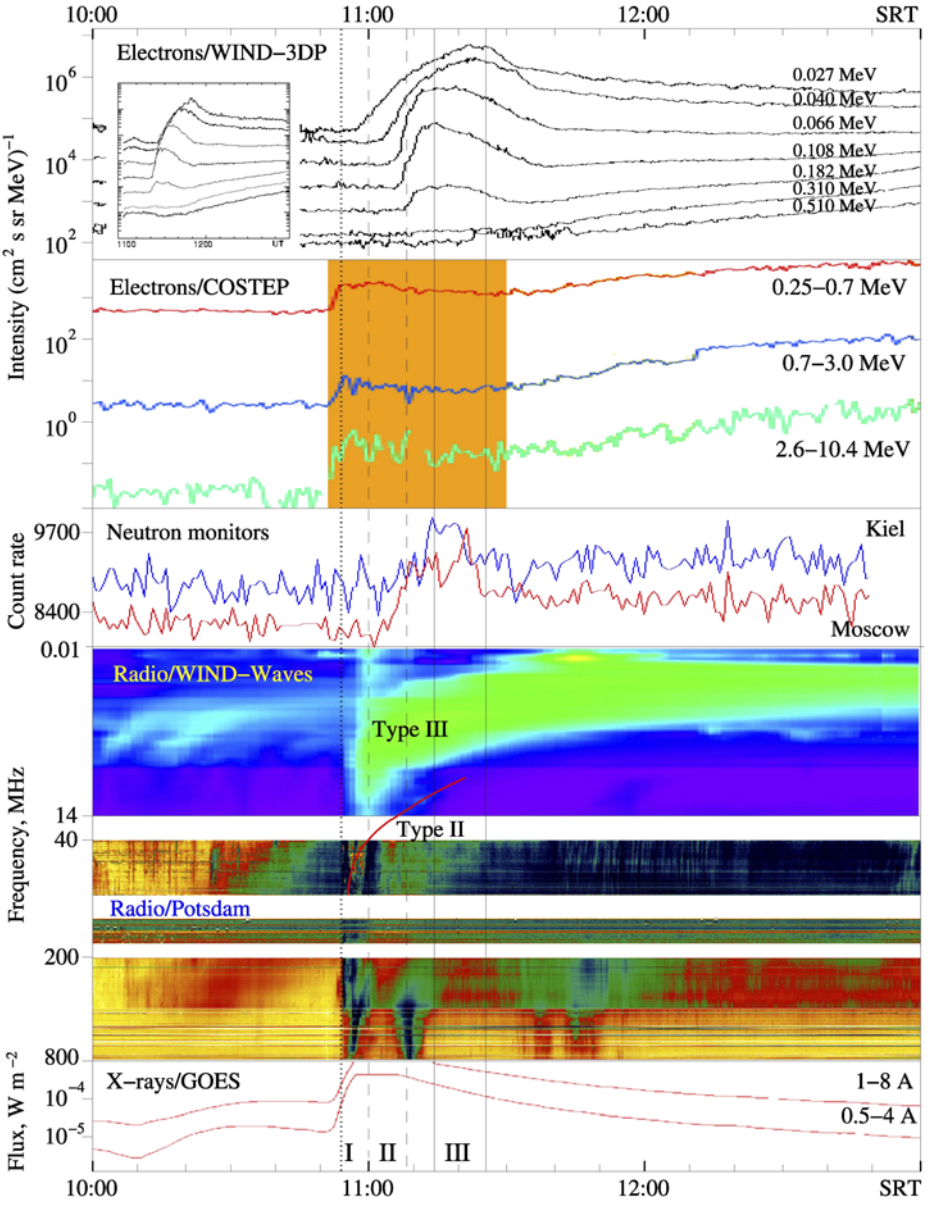

Fig. 1 A large solar NrR and relativistic electron event on 2003 October 28. To remove the effects of electron velocity dispersion all times shown are solar release times obtained by subtracting times of flight. The *top two panels* show the NrR and relativistic electron profiles from the Wind 3DP and SOHO COSTEP instruments, respectively. The inset box shows the 3DP electron channels in real observed time. *Lower panels* show the neutron monitor counting rates, the Wind WAVES and Potsdam radio emission and GOES X-ray flux profiles. The *dashed and solid vertical lines* show inferred solar injection time intervals of an impulsive and gradual electron component, respectively, with respect to the type III burst, shown by the *dotted line*. Other details are given in the figure caption in Klassen et al. (2005)

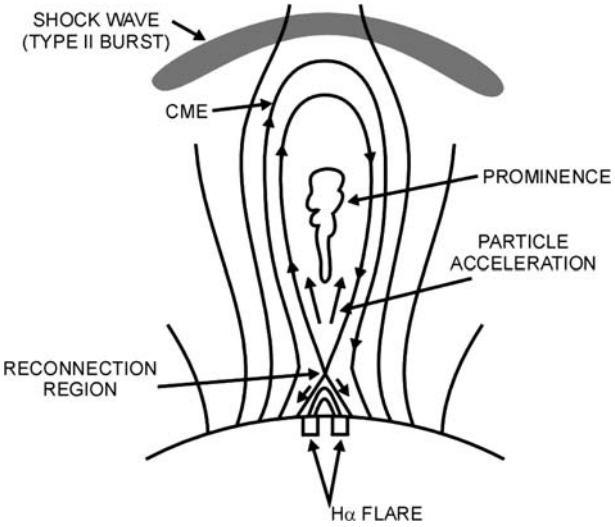

Fig. 2 Schematic showing the coronal flare reconnection region behind a fast CME. Electrons may be accelerated in that relatively confined region or in the much larger region spanned by the CME-driven shock, which produces the radio type II burst. Electrons accelerated over the flare region are assumed to be accelerated on relatively short time scales and to access field lines open to space. Reproduced from Cliver et al. (2004)

of stressed coronal fields that produce hierarchies of stochastic current sheets (Turkmani et al. 2006). Drake et al. (2006) have shown that electrons can undergo Fermi acceleration within the contracting magnetic islands formed in reconnection regions, also resulting in power-law energy distributions. We should keep in mind, however, that a search in solar wind reconnection exhausts has found no evidence for NrR electrons (Gosling et al. 2005), casting doubt on the feasibility of electron acceleration due directly to reconnection.

A long-standing question is how electrons, which have much smaller spatial scale sizes than ions, can be accelerated to high energies at heliospheric shocks (Treumann and Terasawa 2001). Recent work has shown that electron pitch-angle scattering at shock ripples with small size scales (Burgess 2005) and electron cross-field transport at meandering magnetic field lines (Giacalone 2005) allows electron acceleration at quasi-perpendicular shocks. At quasi-parallel (Mann et al. 2001) shocks energization can proceed by multiple electron encounters with large-amplitude magnetic field fluctuations. Solar coronal shocks are produced by coronal mass ejections (CMEs) moving at speeds $v \gtrsim 1000$ km s^{-1}, sufficient to exceed the local MHD fast-mode wave speeds (Gopalswamy et al. 2001a; Mann et al. 2003). Thus, if the heliospheric electrons are accelerated in coronal shocks, they would be injected over the broad longitude ranges ($\gtrsim$60°) of the driver CMEs (Gopalswamy et al. 2001b). Electrons accelerated and injected in solar flares, however, would be observed over a much narrower longitudinal range of ~40° (Reames 1999), probably with impulsive onsets and shorter durations at 1 AU following injections during flare impulsive phases.

Acceleration of electrons to $E > 2$ MeV by traveling shocks has been found in the outer (7–28 AU) heliosphere (Lopate 1989), but in that case the acceleration times can be as long as weeks or months, with most of the acceleration occurring beyond 1 AU. $E > 2$ MeV electrons were also observed from 0.3 to ~35 AU as part of some long-lived ($\gtrsim$27 days) SEP superevents (Dröge et al. 1992), which were attributed to local acceleration in merging systems of CMEs and shocks. A good example of an energetic ($E > 0.3$ MeV) electron spike event at a traveling perpendicular shock was observed on Ulysses at 1.35 AU (Simnett 2003b). Furthermore, $E > 50$ keV electrons produced in heliospheric co-rotating shocks are seen during periods of low solar activity (Roelof et al. 1997;

Simnett 2003a). However, the role of CME shocks as a source of inner heliospheric ($\lesssim$1 AU) NrR and relativistic electron events is not so clear. Here we will assume that the energetic electrons are accelerated either in unspecified impulsive flare processes or in CME-driven shocks, and the question is whether and how we can distinguish flare events from shock events.

It is worthwhile to consider first the analogous acceleration problem for solar energetic ($E \gtrsim 1$ MeV/nuc) proton and ion (SEP) events. The basic paradigm for SEP events is that there are two classes, the impulsive and the gradual events (Reames 1999; Slocum et al. 2003; Tylka and Lee 2006), the former produced near flaring active regions by electric fields or wave–particle interactions (Miller et al. 1997) and the latter in MHD shocks (Lee 2005) driven by fast ($\gtrsim$1000 km s^{-1}) CMEs. Our understanding of these two kinds of ion events has evolved from studies of their very different in situ elemental abundances and ionic charge states, which may be energy-dependent; peak intensities; solar-source longitudes; flare/CME/shock associations; and seed populations (e.g., Tylka et al. 2005). The observations have led to increasingly sophisticated acceleration models dependent on shock geometry and suprathermal seed populations (Tylka and Lee 2006).

The possible observational tools for distinguishing two (or more) kinds or sources of energetic electron events, however, are limited to their in situ energy spectra, pitch-angle distributions (PADs), intensity–time profiles, and the remotely observed solar coronal and interplanetary emissions associated with their coronal injections. Fortunately, most electron events are closely associated with SEP events whose coronal acceleration mechanisms are known or suspected and likely to be common to both the ions and electrons. We review the evidence using these tools, which suggest that CME-driven shocks have an important role in the production of at least some heliospheric energetic electron events. Following a dichotomy of energy ranges based on spacecraft instrumentation, we consider separately observations of the near-relativistic (NrR, $E \gtrsim 30$ keV, $\beta \gtrsim 0.3$) and relativistic ($E \gtrsim 0.3$ MeV, $\beta \gtrsim 0.8$) electron events.

2 Diagnostics for NrR Electron Events

2.1 Solar Injection Onset Times

Although it was long accepted that NrR electrons were injected in type III radio bursts (Lin 1985), which are often signatures of the flare impulsive phase (Bastian et al. 1998), recent observations have indicated coronal injection onsets systematically delayed by ~10 min from the type III bursts or other impulsive phase signatures (e.g., Haggerty et al. 2003; Klein et al. 2005; Fig. 3). The results derive from two similar instruments, the Electron, Proton, and Alpha Monitor (EPAM) on the ACE spacecraft, launched in 1997, and the Solid State Telescope, Foil covered, component of the 3-D Plasma and Energetic Particles instrument (3DP) on the Wind spacecraft, launched in 1994. EPAM covers the approximate energy range 38 to 315 keV with 4 channels (Haggerty and Roelof 2002) and 3DP the range 25 to 500 keV with 7 channels (Ergun et al. 1998). The injection onsets were inferred from the velocity dispersion of the 1 AU onset times, an assumed scatter-free electron propagation, and a 1.2 AU travel distance. Kahler et al. (2007) compared inferred injection times of 80 NrR electron events observed by the 3DP detector with solar 40–800 MHz observations. Other than the preceding type III bursts, no single kind of radio signature characterized the inferred electron injection onset times. In many cases the inferred times matched those of solar brightenings observed in the decametric to decimetric radio range, and this has led to

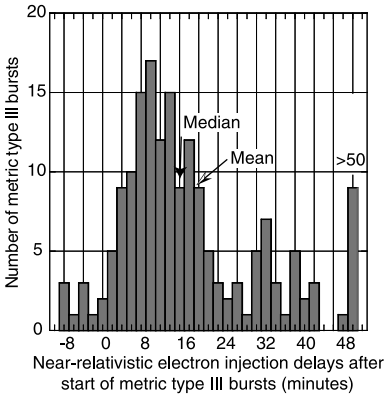

Fig. 3 Distribution of time delays of the inferred solar injections of NrR electrons from the start times of associated flare metric type III radio bursts. The median event delay is 14 min. From Haggerty et al. (2003)

the interpretation of electron acceleration in coronal restructuring in the aftermath of CMEs (Maia and Pick 2004; Klein et al. 2005).

Cane (2003) has argued that the electrons are injected during the times of the type III bursts and that the apparent delays are the result of propagation effects after injection. Supporting her argument was a correlation between the injection delay times and the ambient solar wind densities at 1 AU. This result was also found by Kahler et al. (2007), but in addition both the densities and delay times were inversely correlated with solar wind speeds, suggesting that injection delays increase with longer travel distances, which result from decreasing solar wind speeds.

The 3DP electron injection times are inferred from plots of 1 AU onset times versus c/v, where v is the particle speed. The critical assumptions for those plots and some conflicting SEP-event results from their use have been reviewed by Kahler and Ragot (2006). A basic assumption is that the first-arriving particles propagate scatter-free over field-line lengths of 1.2 AU (Haggerty and Roelof 2002). Recent numerical simulations (Sáiz et al. 2005) have shown that, in most cases, the onset times align close to a straight line as a function of c/v. However, the estimated injection times can be in error by several minutes, and the estimated path length can deviate greatly from the actual path length. Further, turbulent effects result in magnetic field-line wandering to produce field-line lengths substantially longer than 1.2 AU (Ragot 2006). Thus, any insights into electron acceleration derived from comparisons of electron injection times with solar phenomena may be compromised by spurious results of the c/v plot technique. The inferred solar injection times may be correct as most workers assume, or propagation effects may cause some or all times to be inferred incorrectly to be delayed.

2.2 Solar Type II Burst/CME Shock Associations

Solar type II radio bursts in the decametric–hectometric (dh) range are produced by CME driven shocks, usually with speeds $\gtrsim$500 km s^{-1} (Gopalswamy et al. 2001a; Gopalswamy 2004). The origins of metric type II burst shocks can be CMEs, flare ejecta, or flare blast waves (Cliver et al. 1999; Gopalswamy 2004). Flare blast waves have been proposed as minor (Classen and Aurass 2002) or even sole (Vršnak 2001) sources of metric type II bursts. Because CME onsets are generally close in time to the flare impulsive phases, the distinction between flare and CME drivers is difficult to observe. Recent work (Cliver et al. 2005b; Cho et al. 2005; Shanmugaraju et al. 2006) supports the view that CME drivers are the only metric burst sources, as they are for dh type II bursts.

Shock acceleration of electrons can be tested by looking for associations of fast ($\geq$1000 km s^{-1}) CMEs and/or solar type II radio bursts with the 1 AU electron events. Kahler et al. (1994) did a test using $E > 70$ keV electron events and $E > 55$ keV X-rays observed by the Venera-13 and 14 spacecraft. They reasoned that electrons accelerated in shocks would have CME associations and be produced in high coronal regions with low densities and weak X-ray signatures. Those produced in non-shock events, i.e., flares, would not have CME associations and would be produced in lower coronal regions of high densities and strong X-ray signatures. They found that escape efficiencies, defined as ratios of peak electron intensities to X-ray flare fluences, were similar for the event groups with and without CMEs, indicating that CME-driven shock contributions to NrR electron populations were at most comparable to those of non-shock sources.

In a complementary analysis, also pointing to a limited role for shock production of NrR electrons, Klein et al. (2003) examined two cases of type II bursts associated with large hard X-ray flares observed at Ulysses but completely limb-occulted from Earth-orbiting detectors. With a number of necessary assumptions, they showed that the upper limits of $E \gtrsim 30$ keV electrons escaping from the CME-driven shocks of the type II bursts are near the numbers sometimes required in large electron events. Their analysis implies that sources other than the shocks are necessary for the electrons producing long duration X-ray flares and may be important for the interplanetary electron events.

Comparing NrR electron events with associated type II bursts, independently of the burst and injection onset timings, Kahler et al. (2005) showed that metric and decametric type II burst associations were found for only 37% and 17%, respectively, of the electron events. On the other hand, they estimated that ~67% of all metric type II bursts can be associated with observable NrR electron events and that ~50% of the electron events were associated with CMEs sufficiently fast and wide to drive shocks (Gopalswamy et al. 2001b), consistent with the statistics derived from the earlier study by Simnett et al. (2002).

Type II event times and electron injection onsets were then specifically compared by Kahler et al. (2007) to ask whether electron injections occurred during the type II bursts themselves. Almost half the events were associated with metric or decametric–hectometric (dh) type II bursts, but most injections occurred before or after those bursts. Subject to the caveat of spurious injection times (Sect. 2.1), they found that electron injection onsets occurred during type II bursts in at most only 17 of the 80 electron events. Injection onsets relative to CME heights occurred when CMEs were at heights of ~1–5 $R_\odot$, with a median height of 2.4 $R_\odot$ (Haggerty et al. 2003).

Stronger shocks should accelerate electrons to higher energies and perhaps for longer time periods, and this expectation is supported by the correlation found between electron event peak intensities and CME speeds by Simnett et al. (2002) and Haggerty et al. (2003). Their correlations appeared to improve with increasing electron energy. For peak intensities of their 102–175 keV EPAM channel (Fig. 4) we calculate that $r = 0.57$. Gopalswamy et al. (2004) found somewhat lower correlations of $r \sim 0.3$–0.4 for the 3DP peak 108 keV electron intensities versus CME speeds.

Another possible signature of electron shock acceleration is an extended (hours) time of solar injection (see Sect. 3.1), in contrast to an impulsive rise (<1 hr) profile. Beam-like pitch-angle distributions (PADs) at 1 AU may correspond to injection times, depending on the electron scattering characteristics in space. Kahler et al. (2007) compared electron beam-like PAD times with type II burst associations. Only one of their 14 short-duration ($\leq$0.3 hr) beam-PAD events was associated with a metric or decametric type II burst, but 13 of 16 long-duration ($\geq$2 hr) events were associated.

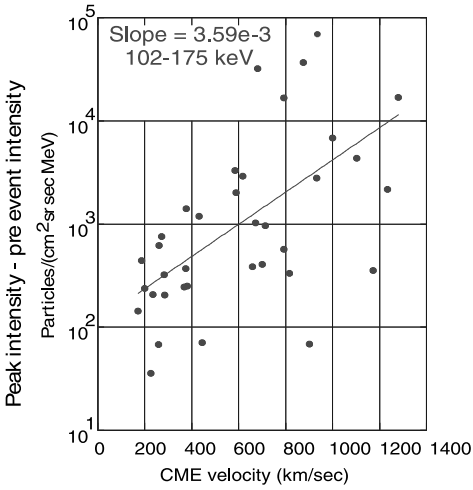

Fig. 4 Peak $102 < E < 175$ keV peak electron intensities versus associated CME speeds, showing a good correlation consistent with shock acceleration of the electrons. From Simnett et al. (2002)

Simnett (2003a) did a similar kind of analysis based on 45 EPAM events selected for fast rise times immediately followed by exponential decays, events most likely to signify impulsive injections. All but 3 events were associated with type III bursts, consistent with impulsive flare injections. Further, of the 23 events with observations from the Large Angle and Spectrometric Coronagraph (LASCO) only 6 could be associated with CMEs with speeds of $v > 650$ km s^{-1}, leading Simnett (2003a) to conclude that CMEs were not required for electron acceleration in those impulsive events. However, CMEs were associated with 14 of those 23 events, and we find that metric type II bursts occurred within 1 hr of 18 of the 45 event onsets, suggesting that even for selected impulsive events shock acceleration could play an important role.

We find that most electron events have no associated shock signatures, suggesting a large population of electron events due only to flares. When associated type II bursts and CMEs are present, it is obviously difficult to distinguish between flare and shock sources for those electron events. Timing criteria for the intensity profiles (Simnett 2003a) or beamed PADs (Kahler et al. 2007) appear promising at this point for making cuts between flare and shock sources of NrR electron events, but resolution of the injection onset delay question (Sect. 2.1) would also be very helpful.

2.3 Solar Flare Flux Associations

Correlations of type II burst and CME parameters with those of electron events can help us judge the likelihood of shock acceleration, but only when compared with similar correlations between flare and electron event parameters. The $E > 70$ keV electron peak intensities correlated well with $E > 55$ keV hard X-ray flare fluences in the Kahler et al. (1994) study. We calculate that $r = 0.69$ for their 17 events. Gopalswamy et al. (2004) found that the 108 keV peak intensities of their electron events correlated at $r \sim 0.6$ with peak soft X-ray flare fluxes. Since their correlation with X-ray flare sizes was better than with CME speeds, Gopalswamy et al. (2004) emphasized the flare sources rather than CME shocks for electron acceleration.

For the peak intensities of their NrR electron events Haggerty and Roelof (2002) found correlations of $r \sim 0.4$ for microwave peak fluxes, ~0.5 for soft X-ray peaks, and ~0.6 for soft X-ray fluences of associated flares. The correlations of electron intensities with CME

speeds (Sect. 2.2; Simnett et al. 2002) were somewhat better than with flare emissions, leading Haggerty and Roelof (2002) to dismiss the flare electromagnetic emissions as "only loosely related" to the electron intensities and favor CME-driven shocks as the electron sources.

Correlations between electron event parameters and those of the associated flares and CMEs can provide at best only a rough guide or consistency check but no details of the physical processes of electron acceleration. Larger flares producing electron events are more likely also to have associated CMEs and type II bursts simply because the flare energetics may scale along with the electron intensities (Kahler 1982). As one might expect, CME speeds correlate with flare soft X-ray fluences (Moon et al. 2002) and peak fluxes (Yashiro et al. 2005; Vršnak et al. 2005) and microwave burst peak intensities (Dougherty et al. 2002). In addition, the CME energies correlate with flare soft X-ray energies (Vršnak et al. 2005). Thus, the electron intensities, CME speeds and flare sizes all scale together statistically and yield no guidance in determining the primary sources of the electron events. In summary, these comparisons of NrR electron events with flare signatures, and with CMEs and type II bursts discussed in Sect. 2.2, suggest an important role for shock acceleration, but they indicate that perhaps most NrR electron events at 1 AU are produced in flares.

2.4 Electron Spectral Variations and CME Associations

Moses et al. (1989) compared soft X-ray flare durations with associated 0.75 keV $< E <$ 100 MeV electron event spectra calculated in units of number density per momentum versus rigidity (momentum). Spectral indices above and below 2 MeV were obtained from observations with separate instruments on ISEE 3, essentially a comparison between NrR and relativistic spectra, for each of 55 electron events. Broken power-law spectra with steep NrR components and flatter relativistic extensions were associated exclusively with short-duration ($\leq$1 hr, SDE) X-ray flares (Fig. 5). The relatively hard, single power-law spectra were associated preferentially with long-duration (>1 hr, LDE) flares. Their results were qualitatively consistent with an inverse correlation between the NrR electron spectral indices and the flare X-ray decay times found by Klecker et al. (1990), but it was remarkable that the spectral distinction was so sharply delineated at the flare duration of 1 hr. The event spectra were later recalculated by Dröge (1996) using true instrumental response functions. He found significant energy shifts and sometimes different spectral shapes compared with those of Moses et al. (1989) but confirmed the basic two-class result. In addition, all spectra showed a flattening below 0.2 MeV, confirming the double power-law shape found in the NrR range for 9 large electron events by Lin et al. (1982).

Moses et al. (1989) preferred to interpret the two classes of electron spectra in terms of differences in coronal heights and densities for electron acceleration. Steinacker et al.

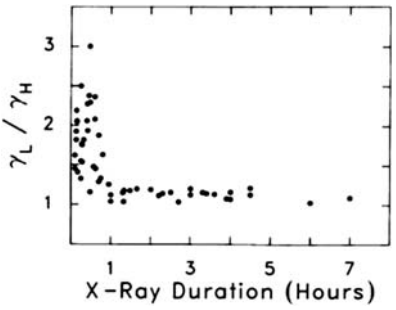

Fig. 5 Broken power-law spectra with steeper NrR ($E < 2$ MeV) exponents γ_L and flatter relativistic ($E > 2$ MeV) exponents γ_H were associated exclusively with short-duration ($\leq$1 hr, SDE) X-ray flares. The relatively hard, single power-law spectra were associated preferentially with long-duration (>1 hr, LDE) flares. From Moses et al. (1989)

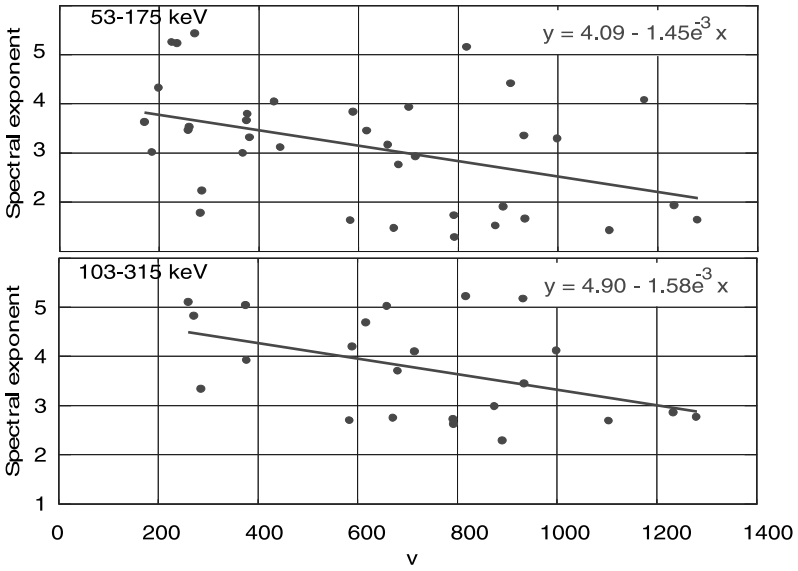

Fig. 6 A correlation between increasing CME speeds v and harder differential-energy spectral exponents γ of associated electron events was found by Simnett et al. (2002). The two-point spectra are flatter with increasing CME speeds. We calculate correlation coefficients $r = 0.42$ and 0.46 for the top and bottom plots, respectively, with a confidence level of >97%. From Simnett et al. (2002)

(1990) assumed only stochastic acceleration in closed loops to model the electron spectra, with Coulomb energy losses at lower heights responsible for the broken power-law spectra of the SDE flares. Moses et al. (1989) also allowed for the possibility of shock acceleration of electrons in the LDEs and, by implication, two classes of electron events. CME associations with flares generally increase with longer flare soft X-ray flux durations (Sheeley et al. 1983; Andrews 2003), so electron acceleration in CME-driven shocks would seem more likely for the LDE flares. However, Kahler et al. (1994) found that of the 19 Moses et al. (1989) events associated with Solwind CMEs, 9 were associated with SDE flares and 10 with LDE flares. They also calculated that the escape efficiencies (ratios of peak electron intensities to X-ray flare fluences) were lower for the LDE than for the SDE flares and that median electron intensities were only somewhat lower for the SDE than for the LDE events. Since the electron events of both the Lin et al. (1982) and Moses et al. (1989) studies were selected on the basis of significant fluxes above ~200 keV and 10 MeV, respectively, they all correspond to the complex events of Lin (1970), which were good candidates for shock acceleration. We might expect the events with the broken power-law spectra to result from additional NrR electron acceleration in the SDE flares. However, Lin et al. (1982) found a good correlation of the $E > 10$ MeV proton energy spectral exponents with those of the NrR $E < 100$ keV electrons, but not with those of the relativistic $E > 0.2$ MeV electrons.

For electron events associated with CMEs a correlation between increasing CME speed and harder electron spectra was found by Simnett et al. (2002, Fig. 6) and confirmed by Haggerty et al. (2003). This result is consistent with the idea that the faster CMEs drive stronger shocks, which accelerate electrons to flatter energy spectra. However, the spectral indices γ of those events, derived from the lowest EPAM energy channels, peak in the range $3 \leq \gamma \leq 4$, similar to the indices of short-duration ($\lesssim$45 min) electron events (Simnett

2005a, 2006b) and to the EPAM events in general (D. Haggerty, priv. comm.), which show no evidence for more than a single class of NrR electron event.

2.5 SEP Event Comparisons

Comparisons of $E \gtrsim 1$ MeV/nucleon ^{3}He-rich SEP events with $E > 19$ keV electron events observed on the ISEE-3 spacecraft showed close associations between the two kinds of events and with type III radio bursts (Reames et al. 1985; Reames and Lin 1985). Reames and Lin (1985) suggested that with greater detection efficiency associated ^{3}He-rich SEP events would be found for all $E > 19$ keV electron events. Since the associations improved with increasing energy, this also suggests good associations between NrR electron events and ^{3}He-rich SEP events. Recent work with the 3DP electron events confirms that ~80% of those events are associated with 0.02–10 MeV nucleon^{-1} ^{3}He-rich (^{3}He/^{4}He $\geq$0.01) events (Wang et al. 2006). Such an association implies NrR electron acceleration along with the ^{3}He-rich ions in flares and not in CME-driven shocks. However, a study of 11 such events (Wang et al. 2005) showed that the ion injections were systematically delayed by ~1 hr relative to the electron injections and that all events were accompanied by west limb CMEs whose origins coincided with electron injection onsets. The majority of the associated CMEs were relatively fast and narrow. That Wang et al. (2005) result is contrary to the simple picture of simultaneous flare acceleration of impulsive ions and NrR electrons and allows the possibility of a shock acceleration of the NrR electrons preceding a later ion acceleration.

Power-law size distributions of electron-event peak intensities can be compared with size distributions of peak flare fluxes and of SEP event peak intensities to determine whether the electron distributions better match the SEP distribution, which is assumed to be a product of shock acceleration. A detailed discussion of the distributions is deferred to Sect. 3.3, but the recent compilation of ~1,100 3DP events (Wang et al. 2006) yields an index $\gamma = 1.34$, similar to $\gamma = 1.3$–1.4 of $E > 10$ MeV SEP events, and less than the $\gamma \sim 1.8$ of flare distributions. The electron event size distribution is therefore more consistent with the presumed shock acceleration of SEPs than with flare production.

A very impulsive and magnetically well connected (W58°) GLE event observed on 2005 January 20 was accompanied by NrR electrons. Simnett (2006a) reported an 06:57 UT electron onset, implying a solar injection delayed by ~6 min from that of the relativistic protons, but this was due to an unfortunate systematic EPAM timing error shown at the EPAM web site (http://sd-www.jhuapl.edu/ACE/EPAM/EPAMtime.pdf). Both the NrR and relativistic electrons were injected within a minute of the relativistic proton injection (Dietrich and Tylka 2006) at ~06:48 UT. This was coincident within ~2 min of the maximum of the flare impulsive phase, but it also corresponded to a time when the associated fast (~2500 km s^{-1}) CME was located at 2–4 $R_\odot$ (Mewaldt et al. 2005; Gopalswamy et al. 2005; Simnett 2006a). Thus, the NrR and relativistic electrons and the relativistic protons were probably all accelerated in a common process, which is consistent with either flare (Simnett 2006a) or shock acceleration. Since the protons are generally presumed to be shock accelerated and the observed ionic charge states are consistent with coronal temperatures (Labrador et al. 2005), the NrR and relativistic electrons must also have been shock accelerated in this unusual event.

2.6 Multiple Spacecraft Observations

Observations of NrR electron events on spacecraft with magnetic connection longitudes far removed from associated solar flare sites are powerful arguments for injections from CME-driven shocks. An early example was a NrR electron event on 1966 July 16 which Dodson et

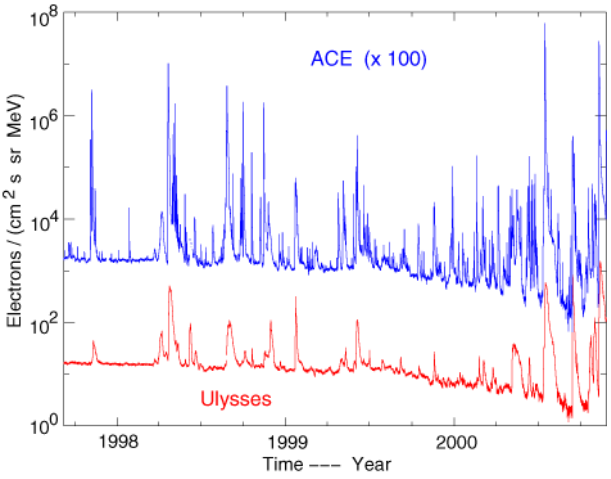

Fig. 7 A comparison of the 175–315 electron keV intensities at ACE (×100) and at Ulysses from 1997 September to 2000 November while Ulysses was climbing from near the ecliptic to heliographic latitude S80°. From Simnett (2003a)

al. (1969) associated with an observed high-latitude eruptive prominence originating from an active region near the back-side central meridian. A more recent example is that of 2001 August 16, which Cliver et al. (2005a) attributed to a halo CME from an active region at ∼W180°.

Comparisons of NrR electron event intensities on widely separated spacecraft can yield angular extents of events and therefore indicate a role for shocks when angular extents are broad ($\gtrsim$100°). Simnett (2003a) has compared NrR electron intensities on EPAM with those from the identical HI-SCALE instrument on the Ulysses spacecraft from 1997 to November 2000 when Ulysses was inbound from 5.4 to 2.2 AU and climbing from the ecliptic to 80° south heliographic latitude (Fig. 7). Despite their large latitudinal and longitudinal separations, all NrR electron events seen at Ulysses were also seen at ACE and are consistent with NrR electron acceleration in CME-driven shocks. Most ACE events, however, do not appear at Ulysses. This could be due either to large radial gradients of the electron intensities that render them unobservable at Ulysses or, more likely, to the narrow source regions in solar flares. The ACE–Ulysses comparison of NrR electrons was extended through the Ulysses fast latitude scan (2000 November to 2001 October) by Maclennan et al. (2003). They also observed electron events at all heliolatitudes, often with Ulysses intensity–time profiles similar to those observed on ACE despite the significant latitudinal and radial separations of the two spacecraft.

Specific Ulysses examples at high (>70°) latitudes are the 5 NrR electron events observed in association with 5 ICMEs shown in Fig. 8. Their associations with both gradual $E \gtrsim 10$ MeV SEPs and ICMEs (Lario et al. 2004) establish them as strong candidates for shock acceleration, although the increased particle intensities inside the ICMEs is not understood. Simnett (2003b) has described a remarkable NrR electron event with an onset time at Ulysses only 6 min after the onset at ACE (Fig. 9). The deduced solar magnetic connection longitudes of W59° at ACE and W192° at Ulysses were separated by 133°, but the solar injections occurred simultaneously at ∼0950 UT on 2001 May 7, in coincidence with a partial halo CME with a speed of $v \gtrsim 600$ km s^{-1}, apparently originating behind the west limb. A second much faster ($v = 1223$ km s^{-1}) CME associated with a C4 X-ray flare at N26° W38° about 2 hr later was followed by a second sharp NrR electron increase at ACE, but only a slight increase at Ulysses. Thereafter there is almost no match in the intensity profiles

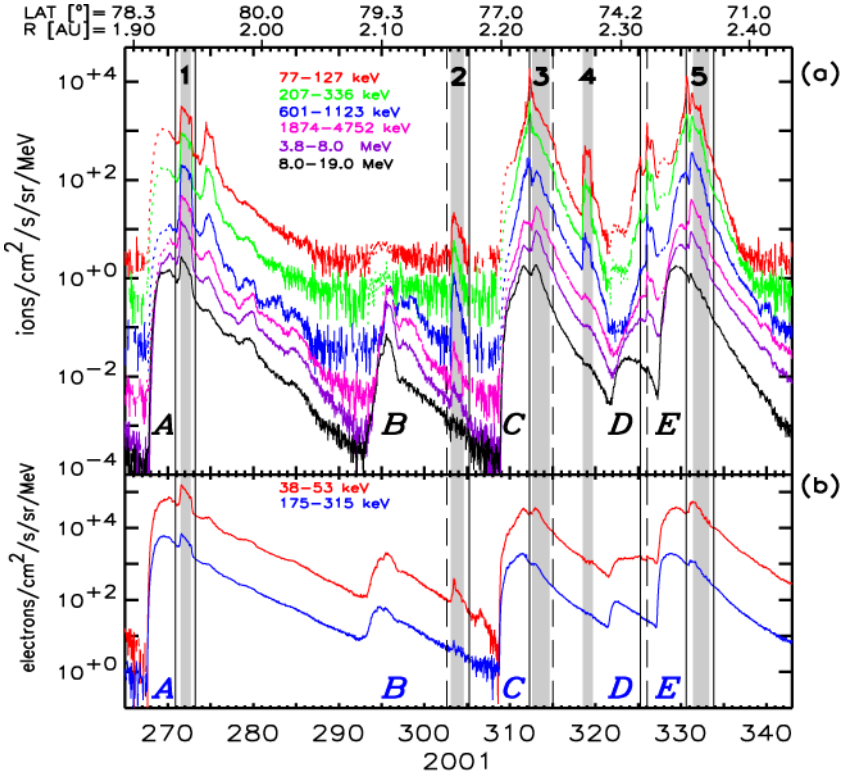

Fig. 8 Five SEP (*top*) and NrR electron (*bottom*) events observed during the northern polar passage of Ulysses at solar maximum in 2001. *Gray bars with numbers* indicate passages of ICMEs. From Lario et al. (2004)

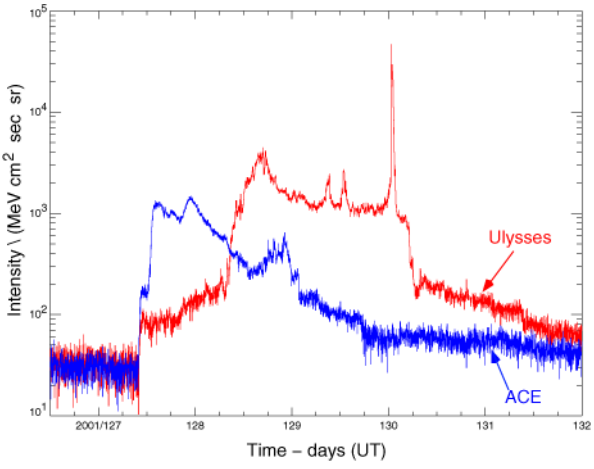

Fig. 9 Comparison of $103 < E < 175$ keV electron intensities at ACE and Ulysses from 2001 May 6 to 11. The event onset at ∼1000 UT on May 7 (DOY 127) at ACE was only 6 min prior to that at Ulysses, located at a solar distance of 1.35 AU. The sharp spike on May 10 accompanied a quasi-perpendicular shock (see Sect. 1). From Simnett (2003b)

of the NrR electrons at the two spacecraft, consistent with more localized solar injections probably due to flare acceleration.

2.7 Coronal Flares

A population of low-energy ($E < 15$ keV) solar electron events with power-law low-energy cutoffs below 2 keV were observed (Potter et al. 1980; Lin 1985) with the ISEE-3 spacecraft. Electron injections from low altitudes in the solar atmosphere were expected to have low-energy cutoffs at higher energies due to Coulomb collisions in the background corona, so those electrons were inferred to be produced in high (>0.5 $R_\odot$) coronal flares (HCFs). The electron events were also statistically poorly associated with signatures of chromospheric flares, but all event onsets coincided with low frequency (<1 MHz) type III bursts (Potter et al. 1980). They have been considered to be a third class of energetic electron event, distinguished from the impulsive flare and second-phase shock-accelerated events (Potter et al. 1980; Robinson and Simnett 2002; Simnett 2005b). Cliver and Kahler (1991) proposed that they originate in current sheet reconnection in streamers.

Robinson and Simnett (2002) suggested that the electron events produced in HCFs may extend to the NrR energy regime. They studied three small NrR electron events observed by EPAM during very low solar activity on 1998 May 5. Those events were characterized by antisunward anisotropies and possible weak dh type III bursts and occurred during the decay of two previous NrR electron events on May 2 and 3 that were associated with large western hemisphere flares and halo CMEs. However, a lack of obvious electron velocity dispersion, the occurrence through the day of a number of small western hemisphere Hα flares, and a possible temporal dependence on several sharp fluctuations in the solar wind speed and magnetic field leave doubt about the origins of the three events.

In a subsequent analysis Simnett (2005b) discussed a series of 9 impulsive NrR electron events that he argued were also produced in HCFs rather than in chromospheric flares. Each event was preceded by a dh type III radio burst, but no reported X-ray or Hα flare, and at most only 3 of the 9 events could be associated with narrow CMEs. Simnett (2005b) therefore proposed, as did Robinson and Simnett (2002), three solar sources of NrR electrons: flares, CME-driven shocks, and the HCFs. However, those 9 NrR events may have been associated with occulted flares in AR 10635 or 10634, on and well over the west limb, respectively. The trend of sequentially decreasing starting frequencies in the associated dh type III bursts is consistent with a source region rotating further over the limb. The event energy spectral indices at peak intensities are somewhat soft, $\gamma \sim 4$–5, but we suggest that these events are also consistent with electron acceleration in occulted solar flares and not in HCFs.

Observations with the 3DP detector revealed NrR electron events whose power-law spectra also extended down to $\sim$0.5 keV (Lin et al. 1996), suggesting an HCF origin for some NrR electron events. There are several arguments against that interpretation, however. First, the event studied by Lin et al. (1996) was associated with a ^{3}He-rich event believed to be produced by hydrogen cyclotron waves, which would be ruled out by the weak magnetic fields at high altitudes (Lin et al. 1996). Second, in a survey of the 3DP NrR electron events after their onsets the in situ electron speed distributions parallel to the magnetic field were rarely plateaued or unstable, even during local Langmuir wave emission (Ergun et al. 1998). This suggests an evolution of the electron velocity distributions, perhaps through interactions with oblique waves such as whistler waves or electromagnetic ion cyclotron waves (Ergun et al. 1998), to maintain the stable distributions. Third, very low-energy ($E < 2$ keV) electron events at 1 AU with observed power-law distributions extending down to at most 142 eV (Gosling et al. 2003) are well associated with metric type III bursts reaching 100 MHz, indicative of origins in high densities of $\sim 10^8$ cm^{-3}. This association is consistent with a low-energy power law established and maintained after leaving the corona.

In our view, HCFs constitute the weakest events in a continuum of first-phase impulsive electron events. Their low total electron energies are matched by weak or undetectable flare signatures. HCFs do not form a third class of electron events at or below the NrR energy range. Lin (1985) pointed out that no clear distinction between HCF and impulsive flare events can be made on the basis of interplanetary observations alone. Gosling et al. (2003) argue that shock acceleration of the $E < 2$ keV electrons in the high corona is unlikely to produce the low energy electron bursts. They suggest that wave interactions will affect the electron spectra seen at 1 AU (Ergun et al. 1998), which would invalidate the original Coulomb energy loss argument. This in turn rescues us from the proposed complexity of electron acceleration in a single electron event occurring over a large range of coronal altitudes and densities (Lin 1993; Lin et al. 1996). In that picture the most tenuous high ($\gtrsim 1$ $R_\odot$) coronal regions must be the sources of the bulk of the energy and numbers of electrons in the power-law spectra. It is likely that all solar electron acceleration is taking place in either flares or shocks, and that HCFs are included in the flares.

2.8 Two-Phase Electron Events—2003 October 28

If there are two or more kinds of electron acceleration and injection in solar events, we might expect to see multi-phase profiles in large NrR electron events. The well studied 2003 October 28 NrR electron event (Fig. 1) is a good candidate. An impulsive component with an injection delayed by 11 min from the type III burst was followed by a gradual component with a harder spectrum (Fig. 10) and delayed by 25 min from the type III burst (Fig. 1). Besides the low-energy ($\leq$30 keV) electrons of the intense type III burst, Klassen et al. (2005) note that the impulsive component injection occurred during decimetric/metric type II and type IV bursts, so it could be attributed to either a shock or coronal magnetic field reconfigurations. They consider that the gradual component is more likely attributable to magnetic reconfiguration behind the shock. Alternatively, Simnett (2005a) interpreted the impulsive component as a result of shock acceleration when the halo CME reached ~5 $R_\odot$ and the gradual component as flare electrons gradually leaking out of a magnetic trap formed by the CME.

A challenge for the October 28 event is to understand how the electrons can be observed at Earth from such a poorly connected (S16°E08°) flare region. Miroshnichenko et al. (2005) noted that the dominant 164 MHz source during the type III bursts lay in the western hemisphere, well away from AR 10486 at E08°. They suggested that the impulsive electrons were

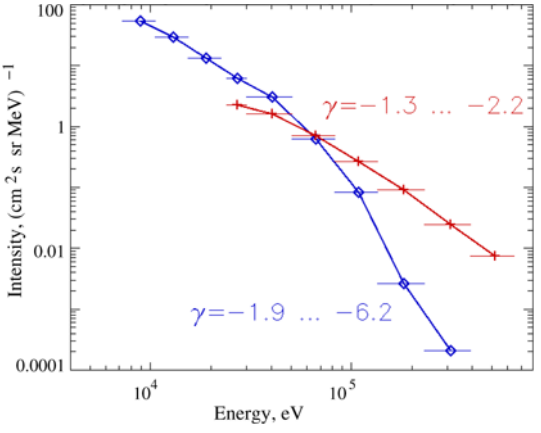

Fig. 10 Energy spectra of the impulsive (*diamonds*) and later gradual (*pluses*) phases during the October 28 event of Fig. 1. Power-law indices γ are given separately for the low-energy ($\leq$40 keV) and high-energy (>66 keV) ranges. From Klassen et al. (2005)

injected into a high-speed stream from the well connected western source region, which also produced the earlier type III radio emission, but after the Earth moved into an ICME connected to AR 10486 the gradual component electrons were injected from the flare site into the eastern footpoint of the ICME loop at 1 AU. The most recent event analysis of Aurass et al. (2006) attributes the impulsive electrons to flare impulsive phase acceleration in a strong termination outflow shock (TS) located SW of AR 10486. TSs are standing fast-mode MHD shocks that occur in the upper and lower outflows of the reconnection region behind the CME (Fig. 2) and may produce type II-like bursts with frequency drift rates implying very low ($<$100 km s^{-1}) speeds (Aurass and Mann 2004). The gradual electron-event source is attributed to evolution of a large current sheet overlying the postflare loop system. Aurass et al. (2006) exclude CME-driven shocks as a significant source of energetic electrons.

Although they differed on the details, all these authors interpreted the October 28 electron event as at least two separate electron injections from different sources and/or acceleration mechanisms. We suggest that the impulsive component was produced in a well connected flare region, and that the gradual electron component was produced in a CME-driven shock, based on its hard energy spectrum and long timescale. This scenario differs significantly from the interpretations offered above, but appears consistent with Lin's (1985) two populations of (1) impulsive 2–100 keV events with single power-law energy spectra from small flares and (2) long-lived $E > 20$ keV events from large flares with harder power-law spectra rolling over at $E \sim 100$ keV. We would attribute the group (2) to CME-driven shocks accompanying the large flares and group (1) to injection during the type III bursts, although the recent interpretations of NrR electron injections invoke time delays from the type III bursts (Sect. 2.1).

Simnett (2006b) has discussed another two-phase NrR electron event observed by EPAM on 2004 February 4. The energy spectrum of the initial beamed pulse was relatively hard ($\gamma = 2.5$) but softer than that ($\gamma = 1.87$) of the gradual component. The event was associated with a well connected Hα flare at W48° and a CME and therefore consistent with the suggested flare/shock two-injection scenario above. A large survey of 45 of the most intense EPAM NrR electron events (Simnett 2006b) found their spectra to be $1 \lesssim \gamma \lesssim 3$, much harder than the $2.5 \lesssim \gamma \lesssim 5.5$ range of 96 pulsed events. The intense events were clearly distinguished from the pulsed events by their higher peak intensities, harder spectra, and longer timescales. Simnett (2006b) preferred to associate the intense events with flares and the pulsed events with CMEs, but as discussed above, we prefer the reverse association. We note that 8 of the 45 intense events were associated with eastern hemisphere flares and 33 of 43 events were associated with fast ($v > 1000$ km s^{-1}) CMEs, which is consistent with event sources in broad CME-driven shocks. A more detailed survey of NrR electron event spectra, intensities, timescales and source regions would be useful for a definitive understanding of the two NrR electron populations.

2.9 Shock-Associated (SA) Events

In Sect. 1, we described the type III and type II radio bursts as signatures of impulsive flare and shock electron acceleration, respectively. With the shocks lasting longer and usually beginning only after flare impulsive phases, we might expect little observational confusion or overlap between the two phenomena. The two flare phases were joined, however, in a controversy, still not settled, over shock-associated (SA) events. These are a class of fast-drift hectometric ($<$2 MHz) events with high intensities and long durations that Cane et al. (1981) and Cane and Stone (1984) reported and interpreted as the merging of low-frequency extensions not of metric type III or microwave bursts but of the herringbone structure of type

II bursts (Fig. 11). The energies of the electrons producing the herringbone and SA events are below the NrR energy range, but the SA events could provide an important signature of the location and duration of shock acceleration of NrR electrons.

The first ensuing controversy about SA (originally termed shock-accelerated to indicate a direct physical connection) events is whether they arise from electrons accelerated in type II burst shocks or are due to impulsive or gradual coronal flare electron acceleration. Statistical studies starting with metric type II bursts (Kahler et al. 1989) and with SA events (MacDowall et al. 1987; Kundu et al. 1990) established only a loose association between the two phenomena. In particular, early components of SA events are generally associated with microwave or type III bursts, leaving only later components possibly associated with type II bursts (MacDowall et al. 1987; Kundu et al. 1990). Klein (1992) and Reiner et al. (2000) compared some SA time profiles with those of associated flare metric and decimetric emission, respectively, and concluded that the SA event electrons escape from coronal flares below any associated type II burst shocks.

A refinement of the SA concept moved the controversy in a new direction. Based on a study of 15 type II bursts with nearly complete frequency coverage from 2 GHz to <0.1 MHz Dulk et al. (2000) defined a class of SA (now shock-*accelerated*) type III bursts, which emanate from type II bursts. They are distinct from the type II herringbone bursts, which have lower beam velocities than type III bursts (Mann and Klassen 2002; 2005). In some cases normal type III bursts appear early, followed by the SA type III bursts, which are defined as having starting frequencies at or less than the simultaneous type II burst frequencies. With this more restrictive definition of an SA event Dulk et al. (2000) concluded

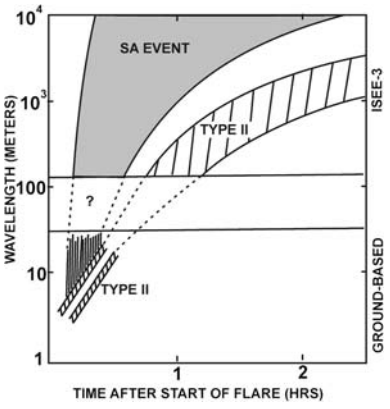

Fig. 11 Schematic illustration of SA events, shown as the shaded region in the hectometric wavelength range of the radiospectrogram. The SA event is presumed to consist of many merged fast-drift bursts extending from the backbone of the type II burst where the electrons are accelerated in the shock. The type II burst may extend into the hectometric range with a separate slow-drift profile. The previous ~2–20 MHz data gap has since been filled by the Wind/WAVES radio experiment. SA events were subsequently redefined as SA type III bursts and type III-*l* bursts. In many cases a metric type III burst preceding the type II burst will also extend into the hectometric range, but those bursts are not considered to be SA events. Crucial for the interpretation of the origin of the SA event/SA type III burst/type III-*l* burst is whether the starting frequencies of the SA events are at (as shown here) or higher (i.e., shorter wavelength) than the type II backbone. From Cane et al. (1981)

that the electrons responsible for SA type III bursts originate in type II shocks and therefore challenged the interpretation of Reiner et al. (2000) and others that all components of SA events can be attributed to flare electrons exclusive of the type II shocks. Aurass et al. (2002) later countered the Dulk et al. (2000) conclusion by suggesting that the interaction of a shock with a streamer could lead to an SA type III burst electron beam not directly due to shock acceleration.

In a study of 123 $E > 20$ MeV SEP events Cane et al. (2002) found that all were preceded by hectometric type III radio bursts, most of which lasted longer than typical type III bursts ($\sim$20 min versus $\sim$5 min) and extended into the times of associated type II bursts. On this basis they introduced the term type III-*l* bursts to replace the previous term, SA events. Whether the type III-*l* burst electrons were shock-accelerated came down to whether the type III-*l* bursts began at the simultaneous type II shock burst frequencies or at higher frequencies characteristic of the underlying flares. A detailed examination of 8 radio spectra showed that the type III-*l* bursts did not originate in type II bursts. Cane et al. (2002) criticized the contradictory Dulk et al. (2000) finding of SA type III bursts originating in type II bursts on the grounds that the Dulk et al. (2000) observations were limited in dynamic range and frequency range. They claimed that many type III bursts occurring later during type II bursts are not reported by observers and that some type II burst features appear to be composed of type III bursts of limited frequencies.

Type III-*l* bursts were qualitatively described by Cane et al. (2002) as being long and intense with a complex profile and occurring more than 10 min after the flare start. MacDowall et al. (2003) deduced a qualitative type III-*l* burst criterion based on hectometric intensity, duration, and complexity that selected for association about 80% of large $E > 10$ MeV SEP events but excluded almost all candidate non-SEP control events. That work, however, did not bear on the question of possible shock production of the type III-*l* burst electrons.

A possible connection between SA type III bursts and NrR electron events was raised in a study by Klassen et al. (2002) of four electron events with type II bursts. Contrary to the Cane et al. (2002) result, they found that the SA type III bursts originated in the type II burst backbones. In all events the inferred NrR electron injections followed SA type III bursts by $>$10 min, so two electron populations were presumed, the first being the low-energy ($<$30 keV) SA type III electrons and the second the NrR electrons. If we assume that the delay times of NrR electrons are incorrect (Sect. 2.1), then there may be NrR electron injections during the SA type III bursts. The NrR electrons would then be directly connected to shock acceleration during type II bursts. Mann et al. (2001) assumed a mirror acceleration of electrons at a parallel shock and achieved good agreement with the observed spectrum of a NrR and relativistic electron event in 1996. Crucial to their interpretation was that the preceding SA type III bursts appeared only at frequencies lower than those of the type II burst. It should be clear that the link from the NrR electrons to type III-*l* bursts (a.k.a. type III SA bursts) to acceleration in type II burst shocks is far from resolved.

3 Diagnostics for Relativistic Electron Events

3.1 Electron Timing Comparisons with CMEs and Flares

The first comparisons of relativistic electron onsets with flare hard X-ray or microwave emission from magnetically well connected flares established that electron injections began within $\pm$1 min of the flare hard X-ray bursts (Bieber et al. 1980; Neustock et al. 1985; Kane et al. 1985). Time–intensity observations of the $E > 0.3$ MeV solar electron events

from the Helios-1 and 2 spacecraft showed that those electron injections were simultaneous with the onsets of the flare hard X-ray and microwave impulsive phases (Fig. 12) (Kallenrode and Wibberenz 1991; Kunow et al. 1991). In a statistical analysis of 27 electron events with ∼15-min time resolution and Helios within 0.5 AU of the Sun, Kallenrode and Svestka (1994) found good agreement between onsets of solar type III bursts and inferred onsets of electron injections. Kane et al. (1985) analyzed an ISEE-3 electron event from a well connected flare on 1982 August 14 and also found that the injection onset occurred during the flare impulsive phase, about 5 min too early to be injected from the observed type II burst shock. Although the intensity profile showed no evidence of a second injection, the strong antisun anisotropy lasted ∼1 hr, consistent with extended shock injection.

Observations at large longitude separations from solar source regions have given good evidence of shock acceleration for relativistic electrons. Early observations by Datlowe (1971) of $E > 12$ MeV electron events on the OGO-V spacecraft following solar flares showed longitude-dependent rise times to intensity maxima similar to those of the associated $E \sim 100$ MeV SEP events (Fig. 13). In the era before the discovery of CMEs (Gosling et al. 1974) he interpreted the longitude dependence in terms of anisotropic diffusion, but today we recognize a CME shock (Reames 1999) as the source of the proton and electron longitude dependence.

A series of studies of $E > 0.3$ MeV electron events observed on the Helios-1 and 2, ISEE-3, Venera-13 and 14, and Phobos-2 spacecraft and associated CMEs observed by the Solwind and SMM coronagraphs were carried out by V. Stolpovskii and colleagues. Each study involved at least 50 electron events observed in the inner heliospheric range of $0.3 < r < 1$ AU. Electron intensities and times were normalized to 1 AU conditions for statistical comparisons with solar X-ray flares and CMEs (Stolpovskii et al. 1995). Selecting 53 electron events associated with both flares and CMEs, Stolpovskii et al. (1997) found that delays of inferred electron injections from solar flare onsets increased substantially outside a longitudinal magnetic footpoint separation range of ±30° (Fig. 14). They modeled the elec-

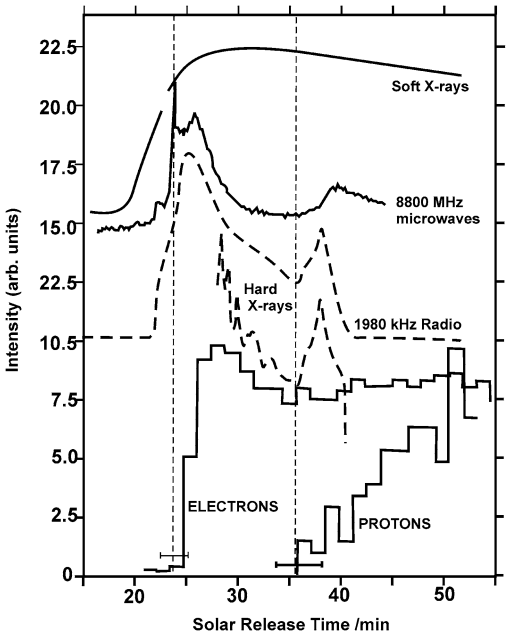

Fig. 12 Time–intensity observations of the $E > 0.3$ MeV solar electron events from the Helios-1 and 2 spacecraft showed that those electron injections were simultaneous with the onsets of the flare hard X-ray and microwave impulsive phases. From Kallenrode and Wibberenz (1991)

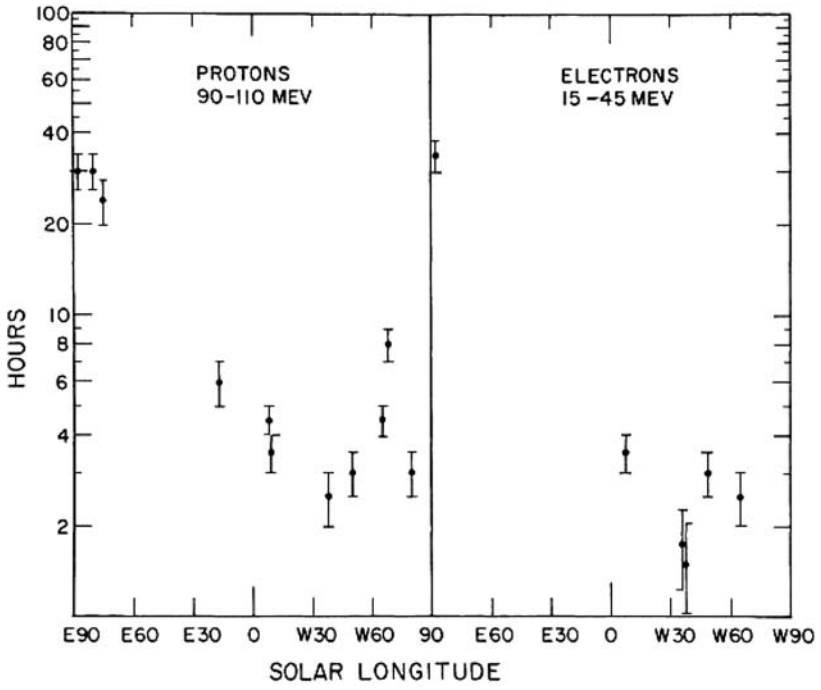

Fig. 13 Times to maximum intensity versus solar flare longitudes for $E \sim 100$ MeV protons (*left*) and $E > 15$ MeV electrons (*right*). From Datlowe (1971)

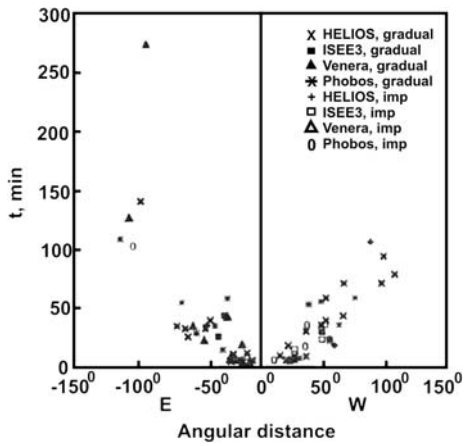

Fig. 14 Delays Δt of the solar injection times of $E > 0.3$ MeV electrons from the start times of 53 associated flares with accompanying CMEs as a function of the longitudinal magnetic footpoint separations ϕ. Symbols distinguish among different spacecraft and between impulsive and gradual flares. Delays increased substantially outside a range of $\pm 30°$ for electron events observed on the Helios and other spacecraft. From Stolpovskii et al. (1997)

tron injection onsets at the times when shocks, propagating away from the flare sites at the observed CME speeds, intersected the magnetic field line connected to the spacecraft. The correlation coefficient between calculated and observed injection delay times was $r \sim 0.8$ for 64 cases, indicating excellent agreement with the model. Their observational results appear consistent with the earlier results of Cliver et al. (1995), who plotted times from solar

flare maxima to electron onsets at spacecraft for extreme longitudinal separations of $\geq 110°$ between the spacecraft and solar flares. Those times ranged from <1 hr to >10 hr.

A shock is expected to populate a given field line with energetic particles as it propagates antisunward along the field line. If the electron production and injection time is longer for faster CME-driven shocks as is assumed for SEPs (e.g., Rice et al. 2003), then the times to reach particle intensity maxima at the observer might also be expected to be longer from faster CMEs and certainly longer than from impulsive injections in solar flares. The electron intensity times to maxima, measured from event onsets to peak intensities and corrected for magnetic angular separation from the associated flare (Schellert et al. 1985), were correlated with associated CME speeds with $r \sim 0.7$ for over 50 events in the reports of Stolpovskii et al. (1997, 1998), consistent with shock sources.

Wibberenz and Cane (2006) selected 19 electron events with short durations and good associations with SDE flares and type III bursts to examine their timing and spatial properties. Each event had to be observed on three spacecraft and have a low e/p ratio indicative of impulsive events, although 10 of the events also had associated type II bursts, suggesting possible shock involvement. They found that the intensity times to maxima were independent of the magnetic longitudinal separations from the associated flares, perhaps consistent with impulsive injections over the event cones of emission.

3.2 Electron Intensity Comparisons with CMEs and Flares

A good statistical connection between 0.2–2 MeV electron events and type III bursts was found by Cane and Reames (1990). They selected electron events associated with strong type III bursts accompanied by type V bursts and found no associated type II bursts for 29 of their 78 electron events, indicating a minimal role for shock acceleration. They suggested that $E > 0.2$ MeV electrons should be detected from all sufficiently intense (>M1) and well connected flares with strong type III/V radio bursts. These studies indicated an important if not dominant role for the flare impulsive phase as the source of relativistic electrons. For electron events observed with Helios spacecraft within 0.5 AU Hucke et al. (1992) found that the electron intensities were not systematically higher when type II bursts were associated with the flares, suggesting minimal shock contribution to the electron intensities, but they examined only electron peak intensities and not the event profiles. Profiles of all 5 electron events of the Kallenrode and Wibberenz (1991) study (Sect. 3.1) were double injections, the second of which occurred during second increases of electromagnetic flare emissions and were characterized by harder spectra than the first injections.

Stolpovskii et al. (1998) found that normalized electron peak intensities of $E > 0.3$ MeV events correlated with peak soft X-ray flare fluxes at about the same level ($r \sim 0.5$) as they did with the associated CME speeds (Sect. 3.1). A similar earlier study of $E > 0.3$ MeV electron events had found a good correlation of $r \sim 0.8$ between the electron peak intensities and the peak solar X-ray flare fluxes for 57 events, with no difference between impulsive and gradual X-ray flares (Stolpovskii et al. 1995). Thus, while the timing characteristics of the electron events support shock injections, the correlations of electron intensities and flare X-ray fluxes are consistent with flare sources.

Solar $E > 0.3$ MeV continuum γ-ray intensities provide a better measure of the flare impulsive phase than do soft X-ray intensities. Klecker et al. (1990) compared peak $E > 0.3$ MeV electron intensities with the calculated number of solar electrons required in a thick-target model to produce the γ-ray fluences for 33 events. They found the ratios of γ-ray electrons to interplanetary electrons to range from ~2 to 200. If the interplanetary

electrons were produced in the flare impulsive phases, then only a small and highly variable fraction of such electrons were escaping.

There are at least two good cases of electron events, on 1981 December 5 (Kahler et al. 1986) and on 1994 April 14 (Veselovsky et al. 1997; Kahler et al. 1998), with associated CMEs but no active region flare involvement. Both electron events were accompanied by $E \gtrsim 40$ MeV SEP events. In neither case was any impulsive flaring activity observed, and although type II bursts were not observed, coronal shock acceleration was considered to be the only reasonable source of the electron event.

3.3 Electron Spectral Variations

Energy spectra of the inner heliospheric electron events were measured in the 0.2 to 3 MeV range and compared for events with and without associated CMEs (Stolpovskii et al. 2001). The FWHM values of the distribution of the integral energy spectral exponent γ were 3.0 and 3.8 for non-CME associated events, and somewhat smaller (harder), 2.2 and 3.4, for those events with CMEs. A clear correlation of harder spectra with faster CMEs was obtained, as shown in Fig. 15. This effect was interpreted as a weakening shock efficiency with decreasing CME speed. In addition, when the angular displacement of the spacecraft magnetic footpoint from the flare site, ϕ, was less than half the CME angular width ψ, suggesting good connection to the shock, the correlation was much tighter ($r \sim 0.8$) and the spectra were harder (bottom panel of Fig. 15) than for all events. The best fit for those events was $\gamma \sim v^{-0.5}$.

Invariant spectra in an ion event occur when all ion species show a spatial invariance in their particular intensities and a single decay time is common to all ions (Reames et al.

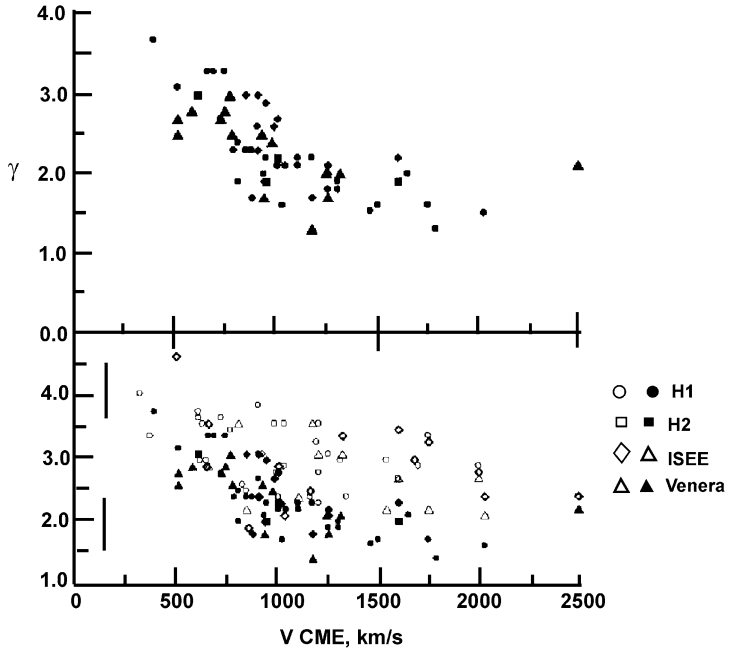

Fig. 15 The exponent γ of the integral power law energy distribution versus associated CME speed V. *Top*: those events for which the separation longitude $\phi < \psi/2$, where ψ is the CME angular width measured in coronagraphs. *Bottom*: All events. From Stolpovskii et al. (2001)

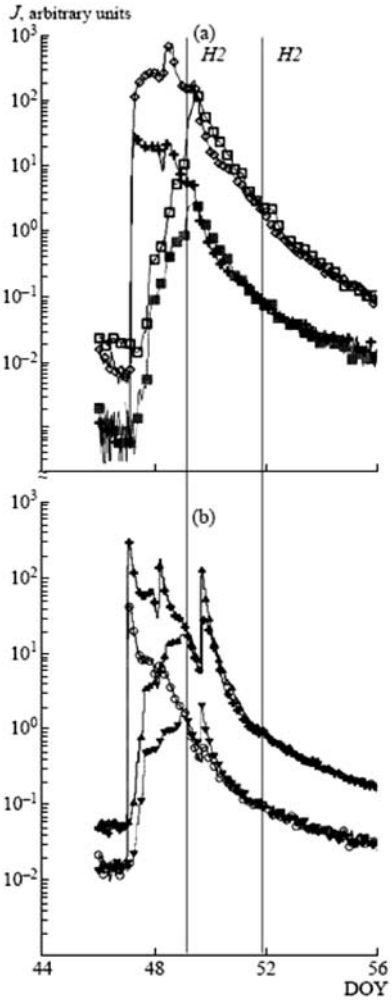

Fig. 16 *Top*: Time–intensity proton profiles in the 16 February 1979 (DOY 47) SEP event. Helios-1 energies are 4–13 MeV (*diamonds*) and 13–27 MeV (*crosses*). The respective Helios-2 data are open and filled squares. *Bottom*: Helios-1 electron energies are 0.3–0.8 MeV (*crosses*) and 0.8–2.0 MeV (*circles*). The respective Helios-2 data are upright and inverted triangles. The passage of the first shock at Helios-2 (*gray vertical line*, *H2*) brings the Helios-2 intensities into the spectral invariant mode along with those of Helios-1. A second impulsive electron event is also observed at both spacecraft late on DOY 49. From Daibog et al. (2003)

1997). The particles are assumed to be quasi-trapped behind the accelerating shock in an expanding bottle and to lose energy by adiabatic deceleration. Particles originating at the western flank of the shock are assumed to be produced in a dynamic quasi-perpendicular shock and have harder spectra (Reames et al. 1997). Invariant spectra were also found by Daibog et al. (2000, 2003) in 17 of 20 $E > 0.3$ MeV and $E > 0.8$ MeV electron enhancements observed simultaneously on Helios-1 and 2 (Fig. 16). Advanced (delayed) onsets of invariance relative to the shock arrivals for spacecraft locations on the eastern (western) flanks of the shocks (Daibog et al. 2003) were similar to those observed for the ions (Fig. 16). While the electrons could be participating in the spectral invariance without an origin in shock acceleration, this similar behavior of electrons and ions strongly suggests that both have a common origin in shocks.

Perhaps more surprising than the invariant spectra is the close agreement of the shapes of the peak energy spectra of events observed on multiple spacecraft with connecting field lines sometimes separated by more than 100° (Dröge 1996). If we assume injections from confined flares, then the electron escape and azimuthal propagation must have little influence

on the spectral shapes (Dröge 1996). If electrons are injected from CME-driven shocks, then the electron injection profiles must be very uniform over the large angular extents. The interpretation in either case provides a serious challenge to our understanding of electron transport.

Flare sources for electrons could be supported by correlations between electron spectra and the inferred spectra of associated flare electrons producing impulsive flare radiation. Dröge (1996) reported a poor correlation between observed and calculated γ-ray spectra when a thick-target model was assumed and a full contribution for the electron spectrum up to 10 MeV was used. By assuming that only the steeper lower-energy (0.2 to 5 MeV) components of the observed SDE and LDE electron spectra (Moses et al. 1989) were responsible for the 0.3 to 1 MeV γ-ray continua, he found that all γ-ray spectral indices lay in the predicted region between thick and thin target models. Further, the LDE spectra were closer to the thin-target model and the SDE spectra to the thick-target model. Dröge (1996) proposed an acceleration model in which a single stage mechanism, such as a shock, produces the lower-energy component of the SDE electrons and the single power-law of the LDE electrons. However, an additional mechanism is needed to produce the high-energy component of the SDE electrons and it is not obvious why the SDE and LDE event exponents should separate toward the thick-target and thin-target fits, respectively.

3.4 Intensity and Timing Comparisons with SEPs

As with the invariant spectra, we can compare properties of electron events with those of associated SEP events whose acceleration processes we think we know. Sufficient event similarities could indicate that both ions and electrons are accelerated in the same process. Kallenrode et al. (1992) compared 0.5 MeV electron and 10 MeV proton events for impulsive (SDE) and gradual (LDE) associated X-ray flares and found the events with SDE flares to be characterized by smaller particle intensities, higher e/p values, smaller ($\pm 50°$ versus $\pm 120°$) cones of emission, and comparable metric type II burst associations. Repeating their work for 19 electron events with SDE flares, Wibberenz and Cane (2006) found the cone of emission to extend somewhat farther, to $\pm 80°$. Fitting a Gaussian profile to the multi-spacecraft intensity peaks yielded a standard deviation of $\sigma = 30°$ in longitude.

$E > 0.5$ MeV electron intensities measured by the EPHIN instrument on SOHO (Sierks et al. 1997) and peak intensities of the associated GOES $E > 10$ MeV protons for impulsive (Reames and Ng 2004) and gradual SEP events were recently compared by Cliver and Ling (2006). The impulsive SEP event sources were predominately confined to the longitude range W20°–W90°. Figure 17 (Cliver and Ling 2006) shows that e/p is highly variable for the impulsive events, but less so for the large well connected gradual events (top) and for the poorly connected gradual events (bottom). The gradual SEP events were also distinguished by their much higher (~90% versus ~20%) associations with dh type II radio bursts and by harder relativistic electron energy spectra than those of the impulsive events. Since the gradual SEPs are assumed to be produced in shocks (Reames 1999), the narrow range of e/p and broad range of source longitudes suggest that the $E > 0.5$ MeV electrons in those events are also produced in shocks along with the ions. In contrast, the large range of e/p for the impulsive events suggests that the relativistic electrons in those events are produced separately from the ions and probably not in shocks.

Assuming that gradual SEP events are produced in shocks, similarities in intensity–time profiles between relativistic electrons and SEPs can provide an argument for shock origins of the electron events. Such a comparison of relativistic electrons with large gradual $E >$ 20 MeV SEP events observed on the Ulysses mission (Sanderson et al. 2003; Sanderson

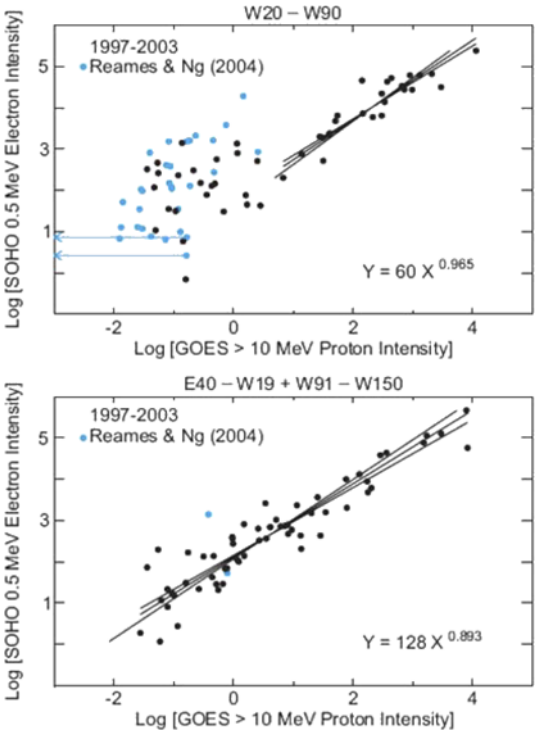

Fig. 17 *Top*: plot of peak 0.5 MeV electron intensities versus peak $E > 10$ MeV proton intensities for well connected SEP events for 1997–2004. A least-squares fit is shown for logs of proton intensities >0.5. *Bottom*: same as top panel, but for poorly connected (E40°–W19° and W91°–W150°) SEP events. Least-squares fit covers the entire intensity range. From Cliver and Ling (2006)

2005) clearly shows (Fig. 18) electron events associated with the gradual SEP events for several different radial distances and heliographic latitudes of Ulysses.

A better case for electron shock acceleration would be made by showing that their solar injection profiles extend well beyond the flare impulsive phase, as is probably the case for the GeV ions of ground-level events (GLEs). For example, Bieber et al. (2005) modeled a $\gtrsim$1-hr injection profile ($\sim$1115 to 1215 UT) for GeV protons of the 2003 October 28 GLE event (Fig. 1), which might match that for the gradual second electron component. Early examples of extended ($\gtrsim$1 hr) electron injection are the events of 1976 March 28 (Bieber et al. 1980) and the 1982 August 14 electron event during a type II burst (Sect. 3.2; Kane et al. 1985). However, more direct comparisons of GeV proton and relativistic electron injections are needed to establish a common acceleration for the two populations.

Hudson (1978) compared statistical event size distributions of flare and SEP peak intensities to determine how SEP production might scale with flare energies. The exponents of the differential power-law distributions $dN/dI \sim I^{-\gamma}$ for flare X-ray and radio burst peaks available at that time, $\gamma \sim 1.8$, have been confirmed by later studies (Crosby et al. 1993, 1998; Bromund et al. 1995; Wheatland 2000; Nita et al. 2002; Su et al. 2006). The smaller exponent of the differential power-law distribution of peak intensities of 40–MeV SEP events, $\gamma = 1.15$ (van Hollebeke et al. 1975), has similarly been found for other SEP energies. The best fits are $\gamma \sim 1.3$–1.4 for $E > 10$ MeV and $E > 100$ MeV events of all longitude source regions (Miroshnichenko et al. 2001; Kahler 2001a; Belov et al. 2005) and $\gamma \sim 1.15$ for magnetically well connected events (Cliver et al. 1991). Hudson (1978) concluded that proportionally greater proton production took place in more energetic flares, but our point of view is that the two different size distributions may serve

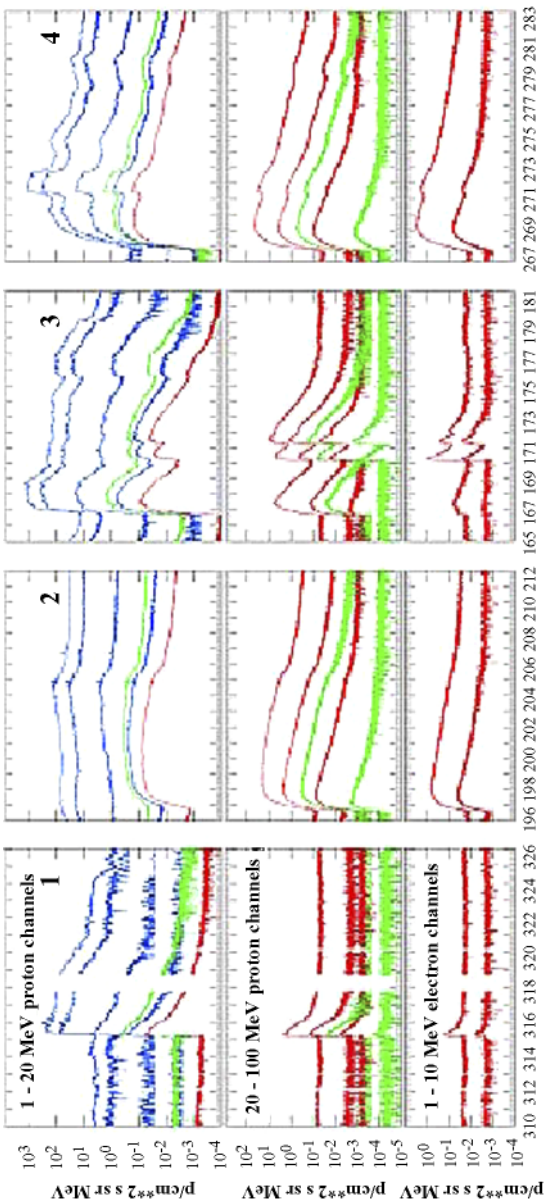

Fig. 18 16-day summary plots for 4 large Ulysses SEP events. For each event the *bottom panel* shows particle intensities from 2 electron channels ranging from 1 to 10 MeV, and the *middle* and *upper panels* show the 1 MeV to 100 MeV SEP profiles. From Sanderson et al. (2003)

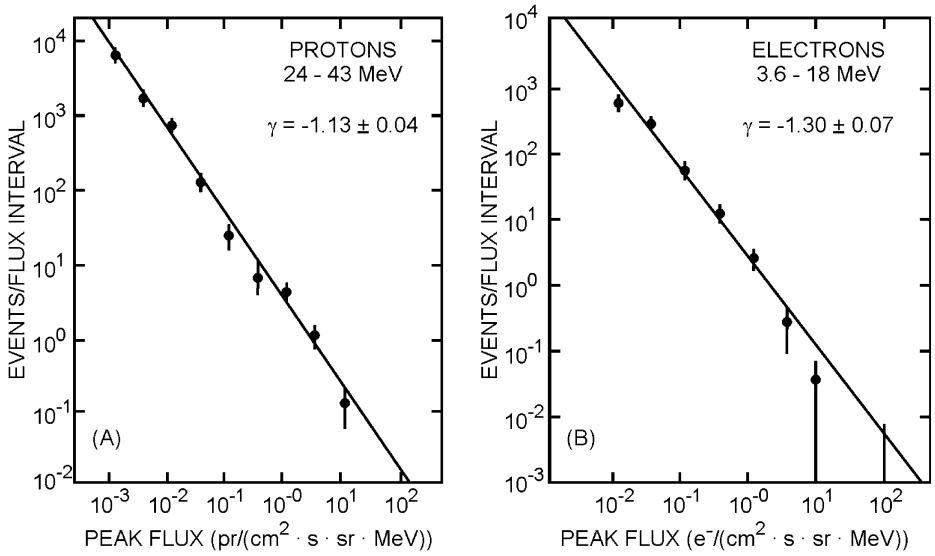

Fig. 19 Size distributions of IMP-8 peak intensities of $24 < E < 43$ MeV proton events (*left*) and $E > 3$ MeV electron events (*right*). From Cliver et al. (1991)

to distinguish the presumed shock acceleration of the SEP events (Cliver et al. 1991) from flare acceleration processes.

We now ask whether recent work on electron peak intensity distributions shows better matches to the SEP distributions than to the flare burst distributions. For well connected $E > 3$ MeV electron events $\gamma = 1.3$–1.4 (Fig. 19; Cliver et al. 1991), steeper than 1.15 for the well connected SEP events, but still lower than ∼1.8 for the flare electromagnetic distributions. Thus the electron event size distribution clearly lies closer to the SEP distributions than to the impulsive flare distributions, so if these distribution differences are indicative of the acceleration processes, then the SEP mechanism of shock acceleration would also be favored over a flare source for the electron events. For flare peak soft X-ray fluxes a further distinction has been found between the power-law size distributions of flares with ($\gamma = 1.98$) and without ($\gamma = 2.52$) associated CMEs (Yashiro et al. 2006). Those γ values are larger than the ones cited above, but still suggest that more energetic flares, i.e., those with CMEs and energetic particles, are somehow different from the lesser energetic flares and are manifested by flatter size distributions. A similar comparison relating impulsive microwave or hard X-ray fluxes to CMEs might be a better discriminator of the electron acceleration process than are the soft X-ray fluxes. A comparison of both SEP and electron size distributions with CME characteristic distributions (Kahler 2001b), such as their speeds or widths, might also prove useful. However, the CME speeds are best fitted with log-normal distributions (Yurchyshyn et al. 2005), in contrast to the power-law fits of flare parameters.

4 Summary

We have reviewed recent work on NrR and relativistic solar electron events at 1 AU to look for evidence of shock acceleration of electrons. For both the NrR (Kahler et al. 2005) and relativistic (Stolpovskii et al. 2001) electron events we have convincing individual cases that

seem to result solely from flares in the absence of either type II bursts or fast CMEs. Also, most NrR electron events are not associated with m/dh type II bursts (Kahler et al. 2005). Those events are therefore unlikely to be produced in coronal shocks. In other events CME-driven coronal shocks appear to be the only reasonable possibility based on the similarity of their intensity-time profiles to those of SEP events and on the extended longitudinal ranges of injection.

Although electron injection from magnetic restructuring after CMEs cannot be ruled out (Sect. 3.1), all solar electron events appear to belong to only two source classes, accelerated either impulsively in solar flares or over longer time scales and larger longitudinal ranges in coronal shocks. The first class includes HCFs, as discussed in Sect. 2.8. This two-class distinction mirrors that of the SEPs (e.g., Tylka and Lee 2006). The primary change from the concept originally proposed by Wild et al. (1963) and Lin (1970) is to extend the impulsive phase energy range to relativistic electrons and to associate some NrR electron events with coronal shocks. The earlier separation of solar classes by energy range no longer holds. However, several decades of observations have not yielded the tools or criteria to make the straightforward class identifications of all 1 AU electron events that we can usually do with SEP events.

There are several approaches that will be helpful in resolving the solar sources of NrR and relativistic electron events. Foremost is the injection timing problem of the NrR electron events (Sect. 2.1); the solar injection times must be correctly inferred before we can compare them with solar event phenomena. Flare impulsive phases are often separated by only minutes from associated CMEs and type II bursts (Leblanc et al. 2001), so the injection timings are a critical tool for associating electron populations with either flares or CME shocks. In addition, comparisons of the energy spectra of the flare microwave and X-ray-producing electrons with those of the interplanetary electrons using microwave and RHESSI observations should prove valuable (e.g., Christe et al. 2005). Such direct comparisons between the two populations have rarely been made (e.g., Pan et al. 1984) and would involve modeling spectral changes during the electron escape process. There is some indication that flare electrons have softer energy spectra than the shock-accelerated electrons, but that is not clear, generally because the NrR and relativistic electron spectra are not yet well characterized. Finally, we should expect to find more electron events with double-phased intensity-time profiles, reflecting separate flare and shock injections. Events such as that of October 28 appear to be rare cases, suggesting that only a single source, flare or shock, is dominant for the great majority of electron events.

Acknowledgements This work was begun during a visit at the Astrophysikalishches Institut Potsdam in 2003 sponsored by the Window on Europe program of the Air Force Office of Scientific Research. I thank E. W. Cliver, H. S. Hudson, and P. Evenson for their helpful critical comments on the manuscript draft.

References

M.D. Andrews, Sol. Phys. **218**, 261 (2003)
H. Aurass, K. Shibasaki, M. Reiner, M. Karlický, Astrophys. J. **567**, 610 (2002)
H. Aurass, G. Mann, Astrophys. J. **615**, 526 (2004)
H. Aurass, G. Mann, G. Rausche, A. Warmuth, Astron. Astrophys. **457**, 681 (2006)
T.S. Bastian, A.O. Benz, D.E. Gary, Ann. Rev. Astron. Astrophys. **36**, 131 (1998)
A. Belov, H. Garcia, V. Kurt, H. Mavromichalaki, M. Gerontidou, Sol. Phys. **229**, 135 (2005)
J.W. Bieber, J.A. Earl, G. Green, H. Kunow, R. Müller-Mellin, G. Wibberenz, J. Geophys. Res. **85**(A5), 2313 (1980)
J.W. Bieber, J. Clem, P. Evenson, R. Pyle, D. Ruffolo, A. Sáiz, Geophys. Res. Lett. **32**, L03S02 (2005). doi:10.1029/2004GL021492

K.R. Bromund, J.M. McTiernan, S.R. Kane, Astrophys. J. **455**, 733 (1995)
D. Burgess, in *The Physics of Collisionless Shocks*, ed. by G. Li, G.P. Zank, C.T. Russell, vol. 781 (AIP, CP, 2005), p. 17
H.V. Cane, Astrophys. J. **598**, 1403 (2003)
H.V. Cane, R.G. Stone, Astrophys. J. **282**, 339 (1984)
H.V. Cane, D.V. Reames, Astrophys. J. Suppl. **73**, 253 (1990)
H.V. Cane, R.G. Stone, J. Fainberg, J.L. Steinberg, S. Hoang, R.T. Stewart, Geophys. Res. Lett. **8**, 1285 (1981)
H.V. Cane, W.C. Erickson, N.P. Prestage, J. Geophys. Res. **107**(A10), 1315 (2002). doi:10.1029/2001JA000320
K.-S. Cho, Y.-J. Moon, M. Dryer, A. Shanmugaraju, C.D. Fry, Y.-H. Kim, S.-C. Bong, Y.-D. Park, J. Geophys. Res. **110**, A12101 (2005). doi:10.1029/2004JA010744
S. Christe, S. Krucker, L. Wang, R.P. Lin, AGU Fall Meeting, abstract #SH31A-04, 2005
H.T. Classen, H. Aurass, Astron. Astrophys. **384**, 1098 (2002)
E. Cliver, S. Kahler, Astrophys. J. **366**, L91 (1991)
E.W. Cliver, A.G. Ling, Astrophys. J. **658** (2007, accepted)
E. Cliver, D. Reames, S. Kahler, H. Cane, in *Proc. 22nd Int. Cosmic Ray Conf.*, Dublin, vol. 3, 1991, p. 25
E.W. Cliver, N.B. Crosby, B.R. Dennis, Astrophys. J. **426**, 767 (1994)
E.W. Cliver, D.F. Webb, R.A. Howard, Sol. Phys. **187**, 89 (1999)
E.W. Cliver, S.W. Kahler, D.V. Reames, Astrophys. J. **605**, 902 (2004)
E.W. Cliver, S.W. Kahler, D.F. Neidig, H.V. Cane, I.G. Richardson, M.-B. Kallenrode, G. Wibberenz, in *Proc. 24th Int. Cosmic Ray Conf.*, Rome, vol. 4, 1995, p. 257
E.W. Cliver, B.J. Thompson, G.R. Lawrence, A.N. Zhukov, A.J. Tylka, W.F. Dietrich, D.V. Reames, M.J. Reiner, R.J. MacDowall, A.G. Kosovichev, A.G. Ling, in *Proc. 29th Int. Cosmic Ray Conf.*, Pune, vol. 1, 2005a, p. 121
E.W. Cliver, N.V. Nitta, B.J. Thompson, J. Zhang, Sol. Phys. **225**, 105 (2005b)
N.B. Crosby, M.J. Aschwanden, B.R. Dennis, Sol. Phys. **143**, 275 (1993)
N. Crosby, N. Vilmer, N. Lund, R. Sunyaev, Astron. Astrophys. **334**, 299 (1998)
E.I. Daibog, V.G. Stolpovskii, S.W. Kahler, Cosm. Res. **41**(2), 128 (2003)
E.I. Daibog, V.G. Stolpovskii, S.I. Svertilov, S.W. Kahler, H. Kunow, G. Erdos, Adv. Space Res. **26**(5), 871 (2000)
S. Dalla, P.K. Browning, Astron. Astrophys. **436**, 1103 (2005)
S. Dalla, P.K. Browning, Astron. Astrophys. **640**, L99 (2006)
D. Datlowe, Sol. Phys. **17**, 436 (1971)
W.F. Dietrich, A.J. Tylka, Eos Trans. AGU, Jt. Assem. Suppl. **87**(36), (2006)
H.W. Dodson, E.R. Hedeman, S.W. Kahler, R.P. Lin, Sol. Phys. **6**, 294 (1969)
B.L. Dougherty, H. Zirin, K. Hsu, Astrophys. J. **577**, 457 (2002)
J.F. Drake, M. Swisdak, H. Che, M.A. Shay, Nature **443**, 553 (2006)
W. Dröge, in *High Energy Solar Physics*, ed. by R. Ramaty, N. Mandzhavidze, X.-M. Hua, vol. 374 (AIP Conf. Proc., 1996), p. 78
W. Dröge, R. Müller-Mellin, E.W. Cliver, Astrophys. J. **387**, L97 (1992)
G.A. Dulk, Y. Leblanc, T.S. Bastian, J.-L. Bougeret, J. Geophys. Res. **105**(A12), 27343 (2000)
R.E. Ergun et al., Astrophys. J. **503**, 435 (1998)
D.J. Forrest, E.L. Chupp, Nature **305**, 291 (1983)
J. Giacalone, in *The Physics of Collisionless Shocks*, ed. by G. Li, G.P. Zank, C.T. Russell, vol. 781 (AIP, CP, 2005), p. 213
N. Gopalswamy, in *The Sun and the Heliosphere as an Integrated System*, ed. by G. Poletto, S.T. Suess (Kluwer, Dordrecht, 2004), p. 201
N. Gopalswamy, A. Lara, M.L. Kaiser, J.-L. Bougeret, J. Geophys. Res. **106**, 25261 (2001a)
N. Gopalswamy, S. Yashiro, M.L. Kaiser, R.A. Howard, J.-L. Bougeret, J. Geophys. Res. **106**, 29219 (2001b)
N. Gopalswamy, S. Yashiro, S. Krucker, G. Stenborg, R.A. Howard, J. Geophys. Res. **109**, A12105 (2004). doi:10.1029/2004JA010602
N. Gopalswamy, H. Xie, S. Yashiro, I. Usoskin, in *Proc. 29th Int. Cosmic Ray Conf.*, Pune, vol. 1, 2005, p. 169
J.T. Gosling, E. Hildner, R.M. MacQueen, R.H. Munro, A.I. Poland, C.L. Ross, J. Geophys. Res. **79**, 4581 (1974)
J.T. Gosling, R.M. Skoug, D.J. McComas, J. Geophys. Res. **30**(13), 1697 (2003). doi:10.1029/2003GL017079
J.T. Gosling, R.M. Skoug, D.K. Haggerty, D.J. McComas, Geophys. Res. Lett. **32**, L14113 (2005). doi:10.1029/2005GL023357
D.K. Haggerty, E.C. Roelof, Astrophys. J. **579**, 841 (2002)

D.K. Haggerty, E.C. Roelof, G.M. Simnett, Adv. Space Res. **32**(12), 2673 (2003)
B. Hamilton, L. Fletcher, K.G. McClements, A. Thyagaraja, Astrophys. J. **625**, 496 (2005)
S. Hucke, M.-B. Kallenrode, G. Wibberenz, Sol. Phys. **142**, 143 (1992)
H. Hudson, Sol. Phys. **57**, 237 (1978)
H. Hudson, J. Ryan, Ann. Rev. Astron. Astrophys. **33**, 239 (1995)
S.W. Kahler, J. Geophys. Res. **87**, 3439 (1982)
S.W. Kahler, J. Geophys. Res. **106**(A10), 20947 (2001a)
S.W. Kahler, in *Space Weather*, ed. by P. Song, H.J. Singer, G.L. Siscoe, AGU Geophys. Mon., vol. 125, 2001b, p. 109
S. Kahler, B.R. Ragot, Astrophys. J. **646**, 634 (2006)
S.W. Kahler, E.W. Cliver, H.V. Cane, R.E. McGuire, R.G. Stone, N.R. Sheeley Jr., Astrophys. J. **302**, 504 (1986)
S.W. Kahler, E.W. Cliver, H.V. Cane, Sol. Phys. **120**, 393 (1989)
S.W. Kahler, E.I. Daibog, V.G. Kurt, V.G. Stolpovskii, Astrophys. J. **422**, 394 (1994)
S.W. Kahler, H.V. Cane, H.S. Hudson, V.G. Kurt, Y.V. Gotselyuk, R.J. MacDowall, V. Bothmer, J. Geophys. Res. **103**(6), 12069 (1998)
S.W. Kahler, H. Aurass, G. Mann, A. Klassen, in *Coronal and Stellar Mass Ejections*, ed. by K.P. Dere, J. Wang, Y. Yan IAU Symp., vol. 226, 2005, p. 338
S.W. Kahler, H. Aurass, G. Mann, A. Klassen, Astrophys. J. **656**, 567 (2007)
M.-B. Kallenrode, Z. Svestka, Sol. Phys. **155**, 121 (1994)
M.-B. Kallenrode, G. Wibberenz, Astrophys. J. **376**, 787 (1991)
M.-M. Kallenrode, E.W. Cliver, G. Wibberenz, Astrophys. J. **391**, 370 (1992)
S.R. Kane, P. Evenson, P. Meyer, Astrophys. J. **299**, L07 (1985)
A. Klassen, V. Bothmer, G. Mann, M.J. Reiner, S. Krucker, A. Vourlidas, H. Kunow, Astron. Astrophys. **385**, 1078 (2002)
A. Klassen, S. Krucker, H. Kunow, R. Muller-Mellin, R. Wimmer-Schweingruber, G. Mann, A. Posner, J. Geophys. Res. **110**, A09S04 (2005). doi:10.1029/2004JA010910
B. Klecker, E. Rieger, D. Hovestadt, D.J. Forrest, E.W. Cliver, W. Dröge, in *Proc. 21st Internat. Cosmic Ray Conf.*, Adelaide, vol. 5, 1990, p. 80
K.-L. Klein, in *Solar Wind Seven*, ed. by E. Marsch, R. Schwenn (Pergamon, Oxford, 1992), p. 635
K.-L. Klein, R.A. Schwartz, J.M. McTiernan, G. Trottet, A. Klassen, A. Lecacheux, Astron. Astrophys. **409**, 317 (2003)
K.-L. Klein, S. Krucker, G. Trottet, S. Hoang, Astron. Astrophys. **431**, 1047 (2005)
M.R. Kundu, R.J. MacDowall, R.G. Stone, Astrophys. Space Sci. **165**, 101 (1990)
H. Kunow, G Wibberenz, G. Green, R. Müller-Mellin, M.-B. Kallenrode, in *Physics of the Inner Heliosphere II*, ed. by R. Schwenn, E. Marsch (Springer, Berlin, 1991), p. 243
A.W. Labrador, R.A. Leske, R.A. Mewaldt, E.C. Stone, T.T. von Rosenvinge, in *Proc. 29th Int. Cosmic Ray Conf.*, Pune, vol. 1, 2005, p. 99
D. Lario, R.B. Decker, E.C. Roelof, D.B. Reisenfeld, T.R. Sanderson, J. Geophys. Res. **109** (2004). doi:10.1029/2003JA010071
Y. Leblanc, G.A. Dulk, A. Vourlidas, J.-L. Bougeret, J. Geophys. Res. **106**(A11), 25301 (2001)
M.A. Lee, Astrophys. J. Suppl. **158**, 38 (2005)
R.P. Lin, Sol. Phys. **12**, 266 (1970)
R.P. Lin, Sol. Phys. **100**, 537 (1985)
R.P. Lin, Adv. Space Res. **13**(9), 265 (1993)
R.P. Lin, R.A. Mewaldt, M.A.I. van Hollebeke, Astrophys. J. **253**, 949 (1982)
R.P. Lin et al., Geophys. Res. Lett. **23**, 1211 (1996)
Y.E. Litvinenko, Sol. Phys. **212**, 379 (2003)
Y.E. Litvinenko, Astron. Astrophys. **452**, 1069 (2006)
C. Lopate, J. Geophys. Res. **94**(A8), 9995 (1989)
R.J. MacDowall, R.G. Stone, M.R. Kundu, Sol. Phys. **111**, 397 (1987)
R.J. MacDowall, A. Lara, P.K. Manoharan, N.V. Nitta, A.M. Rosas, J.L. Bougeret, Geophys. Res. Lett. **30**(12), 8018 (2003). doi:10.1029/2002GL016624
C.G. Maclennan, L.J. Lanzerotti, R.E. Gold, Geophys. Res. Lett. **30** (2003). doi:10.1029/2003GL017080
D.J.F. Maia, M. Pick, Astrophys. J. **609**, 1082 (2004)
G. Mann, A. Klassen, in *Solar Variability: From Core to Outer Frontiers*, ed. by E. Wilson (ESA SP, 2002), p. 245
G. Mann, A. Klassen, Astron. Astrophys. **441**, 319 (2005)
G. Mann, H.-T. Classen, U. Motschmann, J. Geophys. Res. **106**(11), 25323 (2001)
G. Mann, A. Klassen, H. Aurass, H.-T. Classen, Astron. Astrophys. **400**, 329 (2003)

R.A. Mewaldt, M.D. Looper, C.M.S. Cohen, G.M. Mason, D.K. Haggerty, M.I. Desai, A.W. Labrador, R.A. Leske, J.E. Mazur, in *Proc. 29th Int. Cosmic Ray Conf.*, Pune, vol. 1, 2005, p. 111
J.A. Miller, in *High Energy Solar Physics: Anticipating HESSI*, ed. by R. Ramaty, N. Mandzhavidze, ASP Conf. Ser., vol. 206, 2000, p. 145
J.A. Miller, T.N. LaRosa, R.L. Moore, Astrophys. J. **461**, 445 (1996)
J.A. Miller, P.J. Cargill, A.G. Emslie, G.D. Holman, B.R. Dennis, T.N. LaRosa, R.M. Winglee, S.G. Benka, S. Tsuneta, J. Geophys. Res. **102**(A7), 14631 (1997)
L.I. Miroshnichenko, B. Mendoza, E. Pérez, Sol. Phys. **202**, 151 (2001)
L.I. Miroshnichenko, K.-L. Klein, G. Trottet, P. Lantos, E.V. Vashenyuk, Y.V. Balabin, B.B. Gvozdevsky, J. Geophys. Res. **110**, A09S08 (2005). doi:10.1029/2004JA010936
Y.-J. Moon, G.S. Choe, H. Wang, Y.D. Park, N. Gopalswamy, G. Yang, S. Yashiro, Astrophys. J. **581**, 694 (2002)
D. Moses, W. Dröge, P. Meyer, P. Evenson, Astrophys. J. **346**, 523 (1989)
H.-H. Neustock, G. Wibberenz, B. Iwers, in *Proc. 19th Int. Cosmic Ray Conf.*, La Jolla, vol. 4, 1985, p. 102
G.M. Nita, D.E. Gary, L.J. Lanzerotti, D.J. Thomson, Astrophys. J. **570**, 423 (2002)
L.-D. Pan, R.P. Lin, S.R. Kane, Sol. Phys. **91**, 345 (1984)
V. Petrosian, S. Liu, Astrophys. J. **610**, 550 (2004)
D.W. Potter, R.P. Lin, K.A. Anderson, Astrophys. J. **236**, L97 (1980)
B.R. Ragot, Astrophys. J. **653**, 1493 (2006)
D.V. Reames, Space Sci. Rev. **90**, 413 (1999)
D.V. Reames, C.K. Ng, Astrophys. J. **610**, 510 (2004)
D.V. Reames, R.P. Lin, in *Proc. 19th Int. Cosmic Ray Conf.*, La Jolla, vol. 4, 1985, p. 273
D.V. Reames, T.T. von Rosenvinge, R.P. Lin, Astrophys. J. **292**, 716 (1985)
D.V. Reames, S.W. Kahler, C.K. Ng, Astrophys. J. **491**, 414 (1997)
M.J. Reiner, M. Karlický, K. Jiřička, H. Aurass, G. Mann, M.L. Kaiser, Astrophys. J. **530**, 1049 (2000)
W.K.M. Rice, G.P. Zank, G. Li, J. Geophys. Res. **108**(A10), 1369 (2003). doi:10.1029/2002JA009756
I.M. Robinson, G.M. Simnett, J. Geophys. Res. **107** (2002). doi:10.1029/2001JA000305
E.C. Roelof, G.M. Simnett, R.B. Decker, L.J. Lanzerotti, C.G. Maclennan, T.P. Armstrong, R.E. Gold, J. Geophys. Res. **102**, 11251 (1997)
A. Sáiz, P. Evenson, D. Ruffolo, J.W. Bieber, Astrophys. J. **626**, 1131 (2005)
T.R. Sanderson, in *Coronal and Stellar Mass Ejections*, ed. by K.P. Dere, Y. Yan, Proc. IAU Symp., vol. 226, 2005, p. 350
T.R. Sanderson, R.G. Marsden, C. Tranquille, S. Dalla, R.J. Forsyth, J.T. Gosling, R.B. McKibben, Geophys. Res. Lett. **30**, 8036 (2003). doi:10.1029/2003GL017306
A. Shanmugaraju, Y.-J. Moon, K.-S. Cho, M. Dryer, S. Umapathy, Sol. Phys. **233**, 117 (2006)
N.R. Sheeley Jr., R.A. Howard, M.J. Koomen, D.J. Michels, Astrophys. J. **272**, 349 (1983)
G. Schellert, G. Wibberenz, H. Kunow, in *Proc. 19th Int. Cosmic-Ray Conf.*, La Jolla, vol. 4, 1985, p. 305
A.Y. Shih, D.M. Smith, R.P. Lin, G.H. Share, R.J. Murphy, R.A. Schwartz, A.K. Tolbert, AAS SPD meeting #37. AAS Bull. **38**, 220 (2006)
H. Sierks et al., in *Proc. 25th Int. Cosmic Ray Conf.*, Durban, vol. 1, 1997, p. 297
G.M. Simnett, Adv. Space Res. **31**(4), 883 (2003a)
G.M. Simnett, Sol. Phys. **213**, 387 (2003b)
G.M. Simnett, J. Geophys. Res. **110**, A09S01 (2005a). doi:10.1029/2004JA010789
G.M. Simnett, Sol. Phys. **229**, 213 (2005b)
G.M. Simnett, Astron. Astrophys. **445**, 715 (2006a)
G.M. Simnett, Sol. Phys. **237**, 383 (2006b)
G.M. Simnett, E.C. Roelof, D.K. Haggerty, Astrophys. J. **579**, 854 (2002)
P.L. Slocum et al., Astrophys. J. **594**, 592 (2003)
J. Steinacker, W. Dröge, R. Schlickeiser, in *Proc. 21st Int. Cosmic-Ray Conf.*, Adelaide, vol. 5, 1990, p. 32
V.G. Stolpovskii, G. Erdos, S.W. Kahler, E.I. Daibog, Yu.I. Logachev, in *Proc. 24th Int. Cosmic-Ray Conf.*, Rome, vol. 4, 1995, p. 301
V.G. Stolpovskii, E.I. Daibog, S.I. Svertilov, S.W. Kahler, G. Erdos, in *Proc. 25th Int. Cosmic-Ray Conf.*, Durban, vol. 1, 1997, p. 189
V.G. Stolpovskii, E.I. Daibog, S.W. Kahler, G. Erdos, Adv. Space Res. **21**(4), 543 (1998)
V. Stolpovskii, E. Daibog, G. Erdös, S. Kahler, K. Kecskeméty, H. Kunow, in *Proc. 27th Int. Cosmic-Ray Conf.*, Hamburg, vol. 8, 2001, p. 3454
Y. Su, W.Q. Gan, Y.P. Li, Sol. Phys. **238**, 61 (2006)
R.A. Treumann, T. Terasawa, Space Sci. Rev. **99**, 135 (2001)
R. Turkmani, P.J. Cargill, K. Galsgaard, L. Vlahos, H. Isliker, Astron. Astrophys. **449**, 749 (2006)
A.J. Tylka, M.A. Lee, Astrophys. J. **646**, 1319 (2006)

A.J. Tylka, C.M.S. Cohen, W.F. Dietrich, M.A. Lee, C.G. Maclennan, R.A. Mewaldt, C.K. Ng, D.V. Reames, Astrophys. J. **625**, 474 (2005)
M.A. van Hollebeke, L.S. Ma Sung, F.B. McDonald, Sol. Phys. **41**, 189 (1975)
I.S. Veselovsky et al., Cosm. Res. **35**, 119 (1997)
B. Vršnak, J. Geophys. Res. **106**(A11), 25291 (2001)
B. Vršnak, D. Sudar, D. Ruždjak, Astron. Astrophys. **435**, 1149 (2005)
L. Wang, R.P. Lin, S. Krucker, G.M. Mason, in *Proc. Solar Wind 11 - SOHO 16*, vol. 592, ed. by B. Fleck, T.H. Zurbuchen (ESA SP, 2005), p. 457
L. Wang, R.P. Lin, S. Krucker, G.M. Mason, Bull. Am. Astron. Soc. **38**, 256 (2006)
M.S. Wheatland, Astrophys. J. **532**, 1209 (2000)
G. Wibberenz, H.V. Cane, Astrophys. J. **650**, 1199 (2006)
J.P. Wild, S.F. Smerd, A.A. Weiss, Ann. Rev. Astron. Astrophys. **1**, 291 (1963)
S. Yashiro, N. Gopalswamy, S. Akiyama, G. Michalek, R.A. Howard, J. Geophys. Res. **110**, A12S05 (2005). doi:10.1029/2005JA011151
S. Yashiro, S. Akiyama, N. Gopalswamy, R.A. Howard, Astrophys. J. **650**, L143 (2006)
V. Yurchyshyn, S. Yashiro, V. Abramenko, H. Wang, N. Gopalswamy, Astrophys. J. **619**, 599 (2005)